Novel Phenomena Generated by Crystal and Spin Chirality in Solids

Guang-Yu Guo (郭光宇)

Dept. of Physics, National Taiwan University, Taiwan

Physics Div., National Centre for Theoretical Sciences, Taiwan

(Talk in 2nd iTHEMS-NCTS Joint Workshop, RIKEN, Wakoshi, Japan, 18-21 August 2025)

Plan of this Talk

I. Introduction

II. Spin chirality-induced quantum topological Hall effect

III. Topological and chiral phonons in chiral crystals

IV. Crystal chirality and magneto-optical effect in collinear antiferromagnets

V. Summary

I. Introduction

A. Structural chirality

(Structural) chirality (handedness) refers to the asymmetry characterized by non-superimposable mirror images of a material. In chiral crystals, there is no mirror symmetry (*M*) nor spatial inversion symmetry (*P*).

The broken *P*-symmetry enables chiral crystals to exhibit the even-order nonlinear responses to the electromagnetic fields, e.g., nonlinear Hall effect (NLHE), second harmonic generation (SHG) and photogalvanic effect (PGE).

[Sodemann & Fu, PRL 115, 216806 (2015)]

[Ma et al., Nature 565, 337 (2019)]

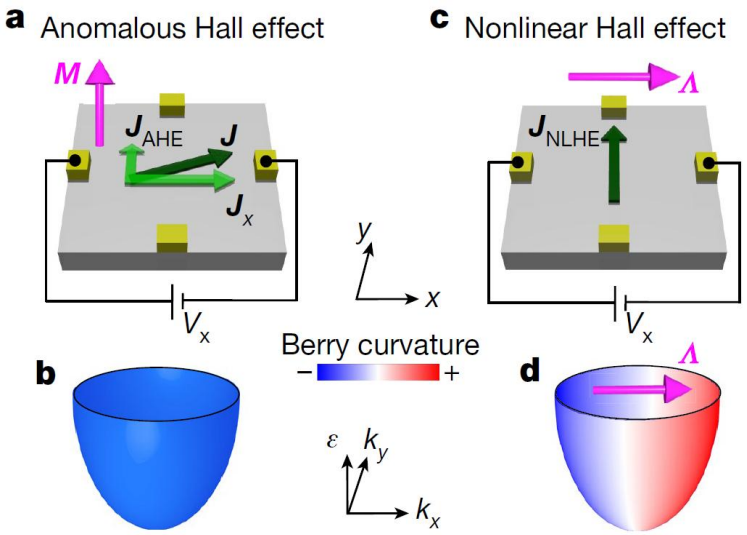

Structural chiral objects

Chiral molecule

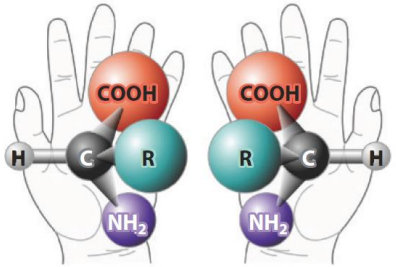

[from Internet]

Chiral crystal

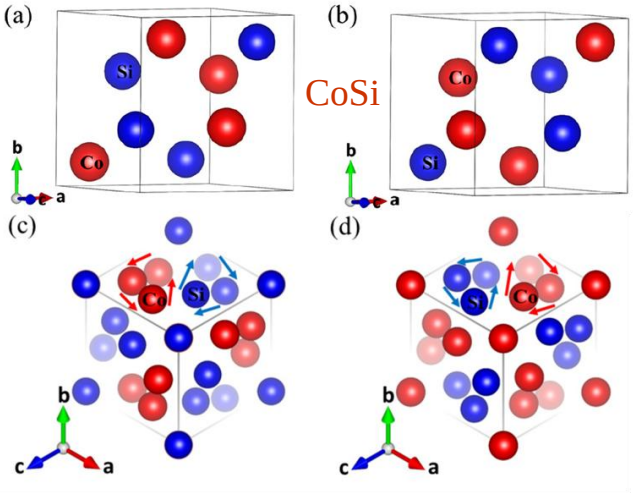

[Hsieh, Prasad, Guo, PRB 106 (2022) 165102]

In addition, chirality enables the chiral crystal to exhibit novel properties, e.g., optical activity (natural circular dichroism) and quantized circular photogalvanic effect (CPGE).

Nonmagnetic Weyl semimetals

[Felser & Gooth, arXiv: 2205.05809 (2022)]

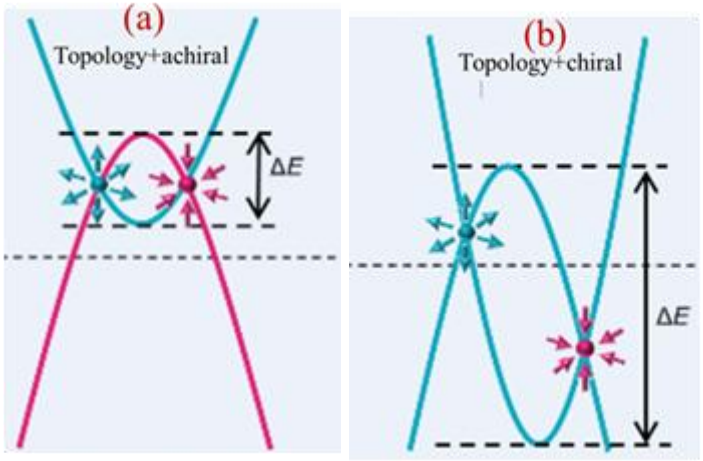

Quantized CPGE in chiral semimetals

[de Juan et al., NC 8 (2017) 15995]

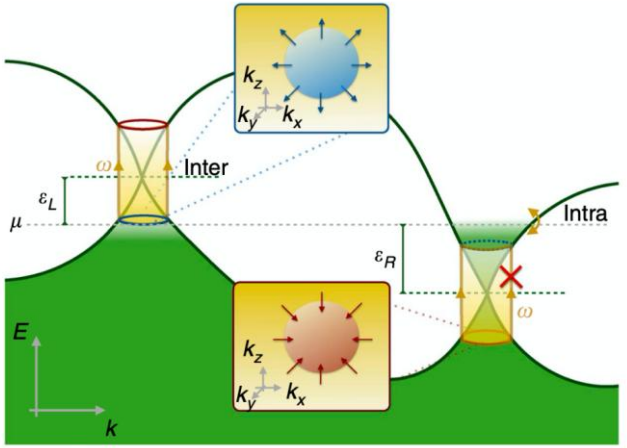

$$\sigma_{inj,C}^{c;ab} = \frac{\tau\pi e^3}{\hbar^2}\int_{\omega_{CV}=\omega}\frac{d^{d-1}k}{(2\pi)^d}(\hat{n}\cdot\hat{c})F^{ba},$$

$F^{ba} = -2\,\mathrm{Im}(r_{CV}^{b} r_{VC}^{a})$ is the Berry curvature.

For a single Weyl cone,

$$\frac{1}{2\pi}\int_{\omega_{CV}=\omega}\frac{d^{d-1}k}{(2\pi)^d}(\hat{n}\cdot\hat{c})F^{ba} = C,$$

C is the chiral charge of the Weyl node.

In chiral Weyl semimetals, the energy levels of the Weyl nodes may be different, and thus quantized CPGE may occur.

B. Spin chirality

Spin chirality refers to a multispin quantity representing the sense (handedness) of the noncollinear spin structures induced by spin frustration. There are two types of spin chirality, viz, vector spin chirality in, e.g., noncollinear and coplanar spin structures (Fig. 1) and scalar spin chirality in noncoplanar spin structures (Fig. 2).

[Kawamura, Can. J. Phys. 79 (2001) 1447]

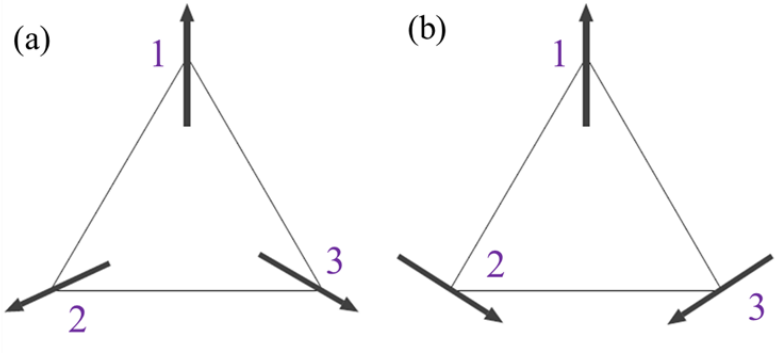

Fig. 1 Two chiral states in the (a) right- and (b) left-handed structures of three coplanar spins on a triangle. The nonzero vector spin chirality (an axial vector) is $\boldsymbol{\kappa} = \frac{2}{3\sqrt{3}} \sum_{<ij>} \mathbf{S}_i \times \mathbf{S}_i .$

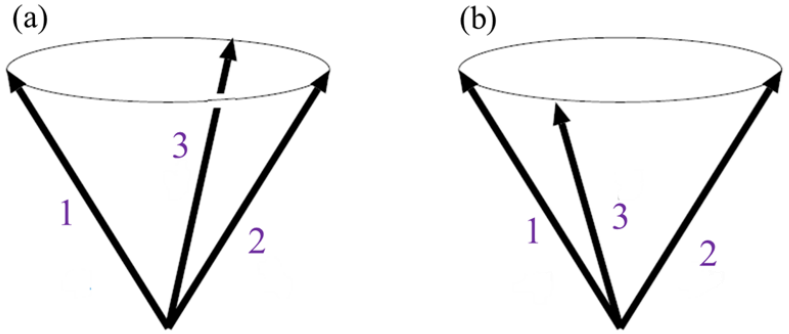

Fig. 2 Two chiral states in the noncoplanar spin structure formed by three spins. The nonzero scalar spin chirality (a pseudoscalar) is defined by $\chi = \mathbf{S}_i \cdot (\mathbf{S}_j \times \mathbf{S}_k).$

Examples of the chiral spin structures of the 1st and 2nd types include the 3D stacked-triangular lattice (Fig. 1) and the skyrmion lattice (Fig. 2)], respectively.

[Feng et al., PRB 92 (2015) 144426]

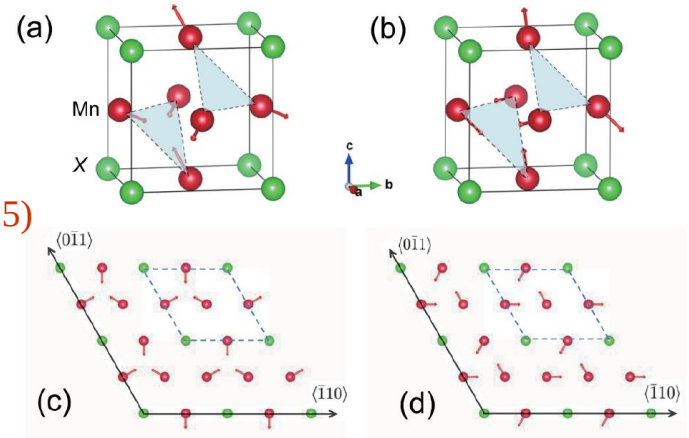

Fig. 1 Noncollinear coplanar (a) T_1 and (b) T_2 antiferromagnetic structures with vector spin chirality of cubic Mn_3X (X = Rh,Ir,Pt).

[Fujishiro et al., NC 10 (2019) 1059]

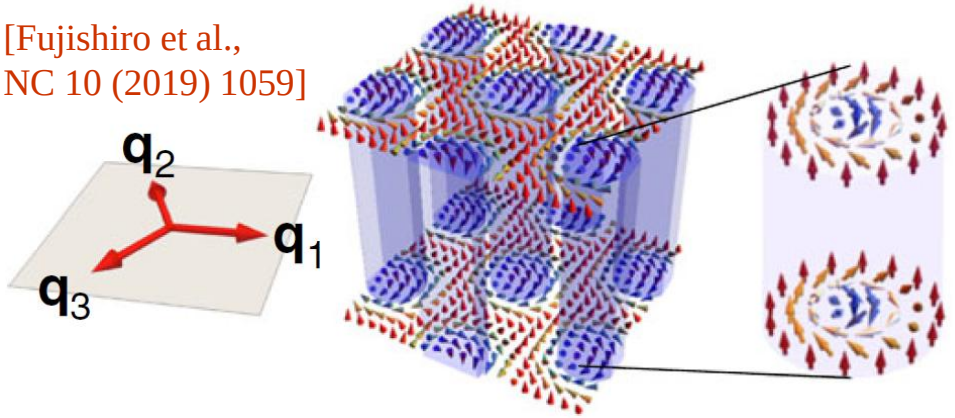

Fig. 2 A skyrmion lattice with scalar spin chirality in Noncollinear coplanar antiferromagnetic structures of chiral magnets $MnSi_{1-x}Ge_x$.

Spin chirality could play an important role in the magnetic ordering of frustrated systems and could cause surprising phenomena, e.g., the anomalous Hall effect and magneto-optical Kerr effect in noncollinear antiferromagnets Mn_3X (Figs. 1, 3 and 4).

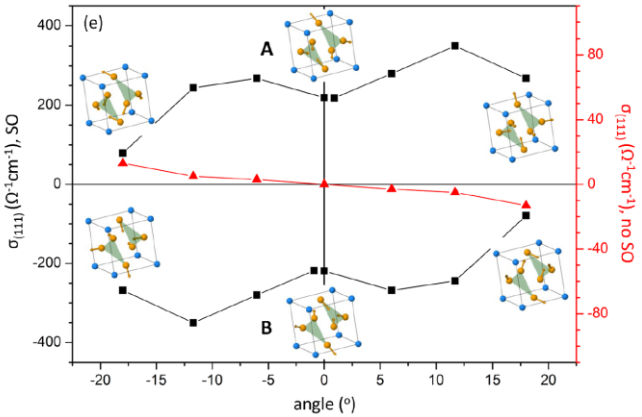

[Chen, Niu & MacDonald, PRL 112 (2014) 017205]

Fig. 3 AHE in Mn_3X (X = Rh, Ir, Pt).

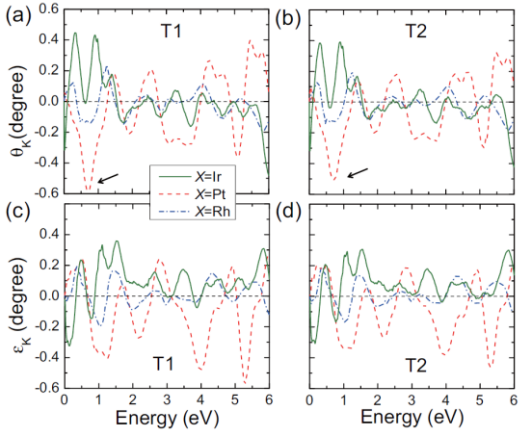

[Feng et al., PRB 92 (2015) 144426]

Fig. 4 MOKE in Mn_3X (X = Rh, Ir, Pt).

II. Spin chirality-induced quantum topological Hall effect

A. Scalar spin chirality and topological Hall effect

The anomalous Hall effect (AHE) [Hall 1881] in ferromagnetic metals has been attributed to the nonzero magnetization and spin-orbit coupling (SOC).

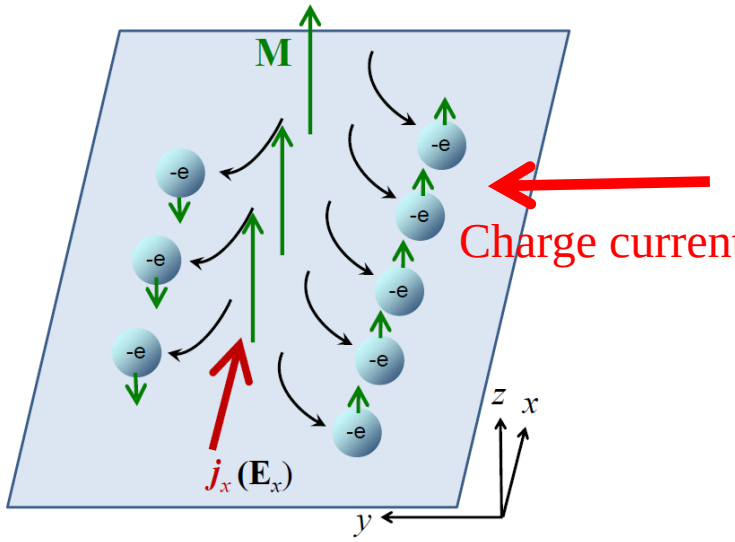

Mn_5Ge_3

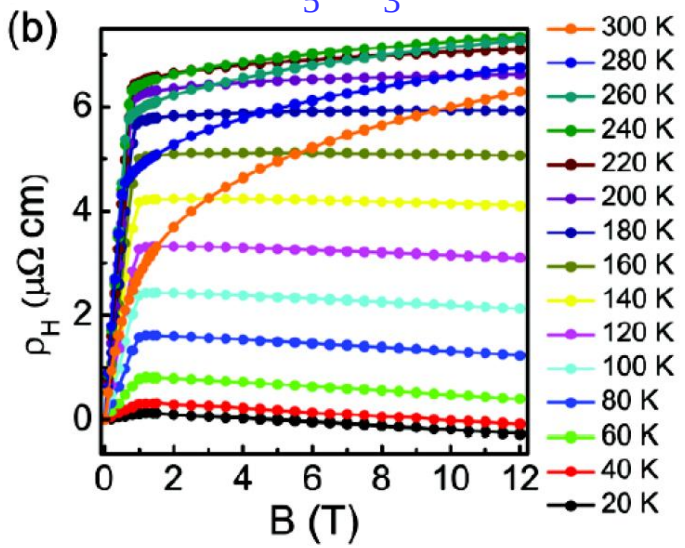

[Zeng et al. PRL 96 (2006) 2010]

$$\rho_H = R_0 B + R_S M$$

Furthermore, this can be explained in terms of Berry curvature (**Ω**) in **k**-space.

1) **Ω** produces anomalous velocity

$$\dot{\mathbf{x}}_c = \frac{1}{\hbar}\frac{\partial \varepsilon_n(\mathbf{k})}{\partial \mathbf{k}} + \frac{e}{\hbar}\mathbf{E}\times\mathbf{\Omega}_n(\mathbf{k}),$$

$$\mathbf{\Omega}_n(\mathbf{k}) = -\,\mathrm{Im}\left\langle \frac{\partial u_{n\mathbf{k}}}{\partial \mathbf{k}} \right| \times \left| \frac{\partial u_{n\mathbf{k}}}{\partial \mathbf{k}} \right\rangle.$$

[Xiao, Chang & Niu, RMP 82, 1959 (2010)]

2) Semiclassical transport theory

$$\mathbf{j} = \int d^3k(-e\dot{\mathbf{x}})(f(\mathbf{k}) + \delta(\mathbf{r},\mathbf{k})),$$

$$\mathbf{j} = -\mathbf{E}\times\frac{e^2}{\hbar}\int d^3\mathbf{k} f(\mathbf{k})\mathbf{\Omega} - \frac{e}{\hbar}\int d^3\mathbf{k}\delta f(\mathbf{k},\mathbf{r})\frac{\partial \varepsilon_n(\mathbf{k})}{\partial \mathbf{k}}$$

(Hall conductance)

Surprisingly, AHE was observed in noncoplanar antiferromagnets.

This could be explained as the topological Hall effect (THE) driven by scalar spin chirality.

[Taguchi et al., Science 291, 2573 (2001)]
[Tatara, Kawamura, JPSJ 71 (2002) 2613]
[Nagaosa, JPSJ 75 (2006) 042001]

Consider a double exchange model

$$H = -\sum_{ij,\alpha} t_{ij}(c^{\dagger}_{i\alpha}c_{j\alpha} + h.c.) - J_H \sum_i S_i \cdot c^{\dagger}_{i\alpha}\sigma_{\alpha\beta}c_{i\beta}.$$

In the limit $J_H \to \infty$, the conduction electron spin is forced to align parallel to the localized spin at each site.

$t_{ij}^{eff} = t_{ij}e^{ia_{ij}} \cos(\theta_{ij}/2)$, where
θ_{ij} is the angle between $\mathbf{S}_i$ and $\mathbf{S}_j$.

The resultant $\sigma_{xy} \propto \chi_0$ where

$$\chi_0 = \frac{1}{6N}\sum_i \mathbf{S}_i \cdot (\mathbf{S}_{i+1} \times \mathbf{S}_{i+2}).$$

[Taguchi et al., Science 291, 2573 (2001)]

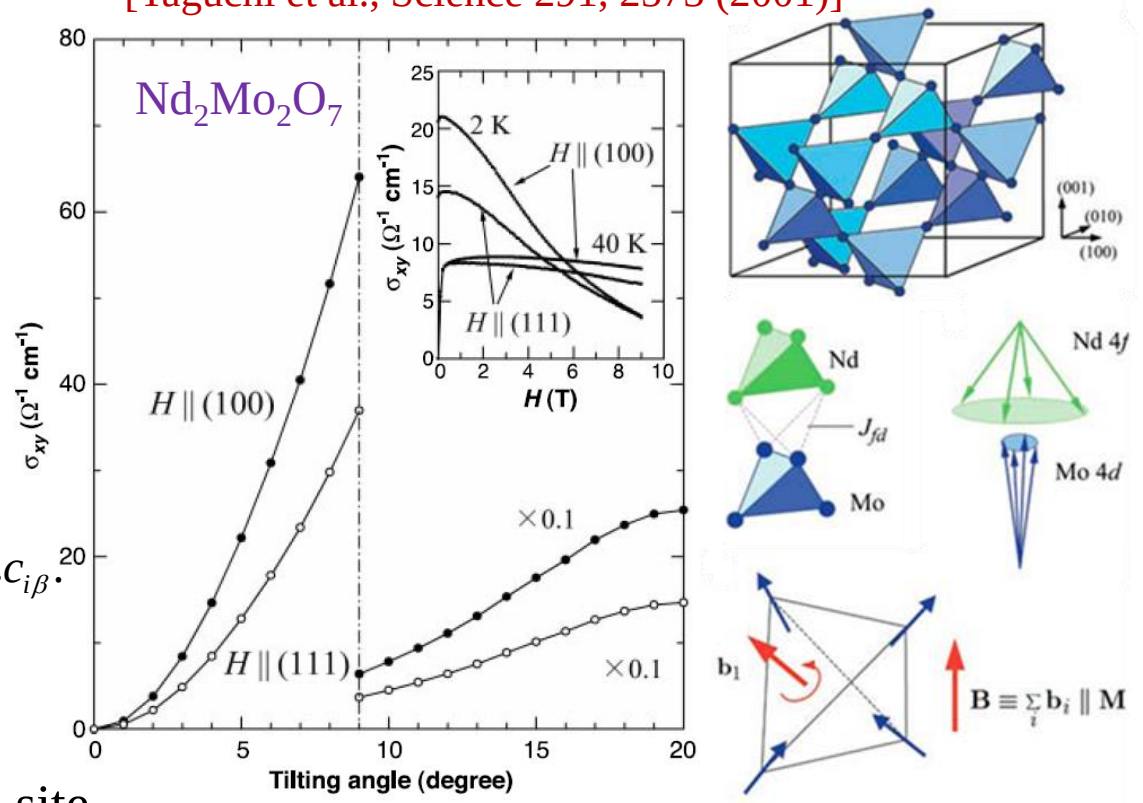

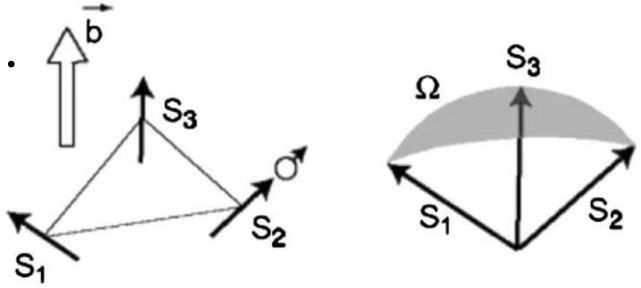

Fig. 1 An electron moving around three noncoplanar spins, feels a fictitious magnetic field **b** with the flux given by the half of the solid angle Ω subtended by the three spins.

B. Chiral noncoplanar antiferromagnetism in layered oxide $K_{1/2}RhO_2$

$K_{1/2}RhO_2$ has a layered hexagonal γ-Na_xCoO_2-type structure ($P6_3/mmc$) with two 1T-RhO_2 layers stacked along *c*-axis [2f.u./cell]. [Shibasaki et al., JPCM 22 (2010) 115603]

All possible magnetic structures in 2×2×1 supercell.
[Zhou et al., PRL 116, 256601 (2016)]

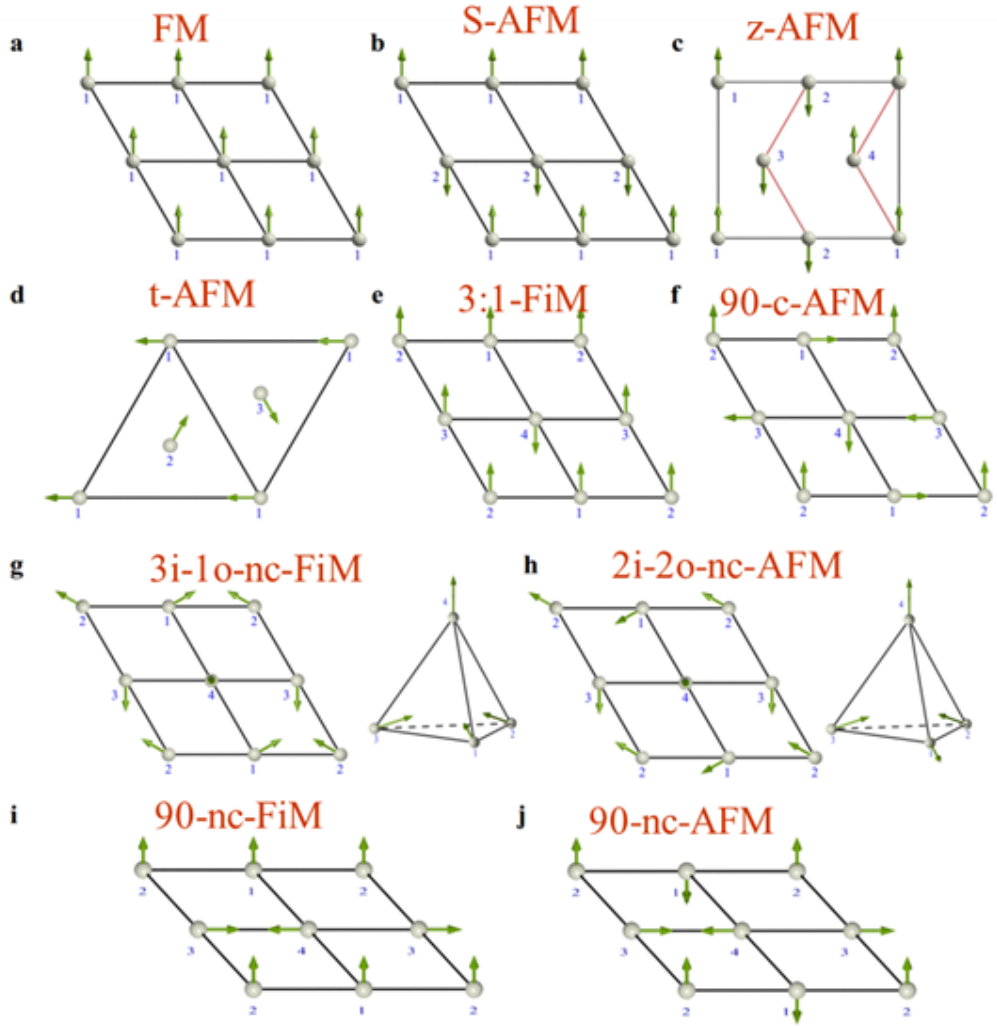

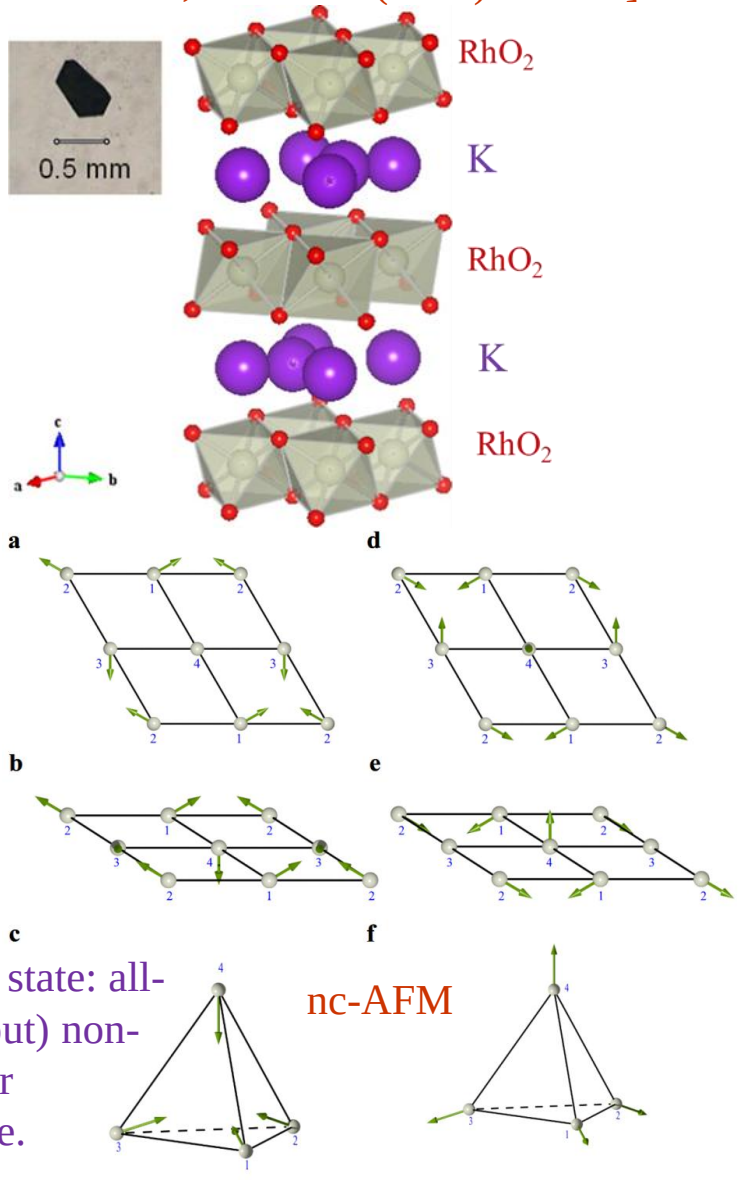

Ground state: all-in (all-out) non-coplanar structure.

nc-AFM

Total energy (ΔE^{tot}) (meV/f.u.), total spin moment (m_s^{tot}) (μ_B/f.u.), Rh atomic spin moment (m_s^{Rh}) (μ_B/f.u.) and band gap (E_g), from GGA+U calculations.

[Zhou et al., PRL 116, 256601 (2016)]

	ΔE^{tot}	m_s^{tot}	m_s^{Rh}	E_g
NM	20.19	0.00	0.00	metal
FM	2.48	0.50	0.36	metal
s-AFM	5.61	0.00	0.23	metal
z-AFM	12.85	0.00	0.23	metal
t-AFM	20.17	0.00	0.10	metal
3:1-FiM	1.99	0.00	0.06/0.15/0.24/-0.47	metal
90-c-AFM	2.20	0.00	0.23	metal
90-nc-AFM	2.14	0.00	0.23	metal
nc-AFM	0.00	0.00	0.24	0.22

Ground state: all-in (all-out) noncoplanar antiferromagnetic structure, a semiconductor with a small band gap of 0.22 eV.

Heisenberg model

$$H = E_0 - \sum_{i<j} J_{ij}\sigma_i \cdot \sigma_j$$

Exchange coupling

$J_1 = 4.4$, $J_2 = -3.6$ meV

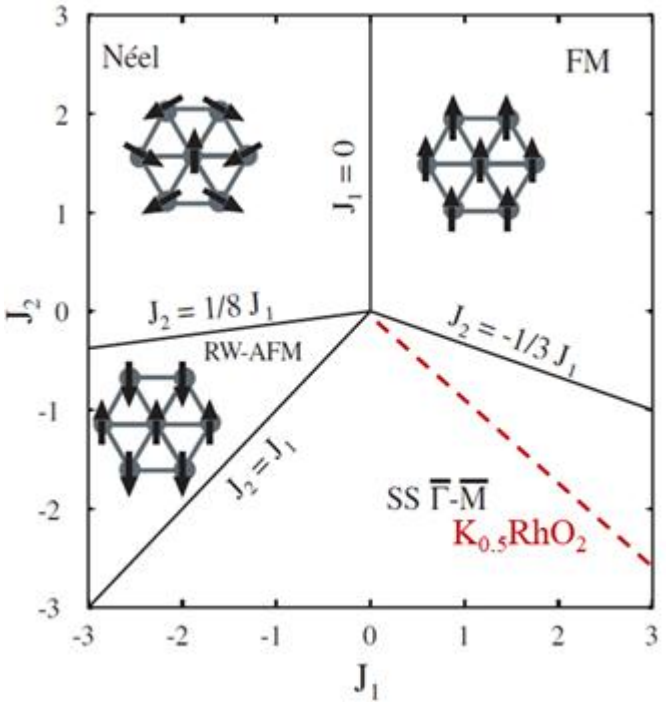

[Henze et al., APA 75, 25 (2002)]

C. Exotic quantum topological Hall phase

(1) A Chern insulator

[Zhou et al., PRL 116, 256601 (2016)]

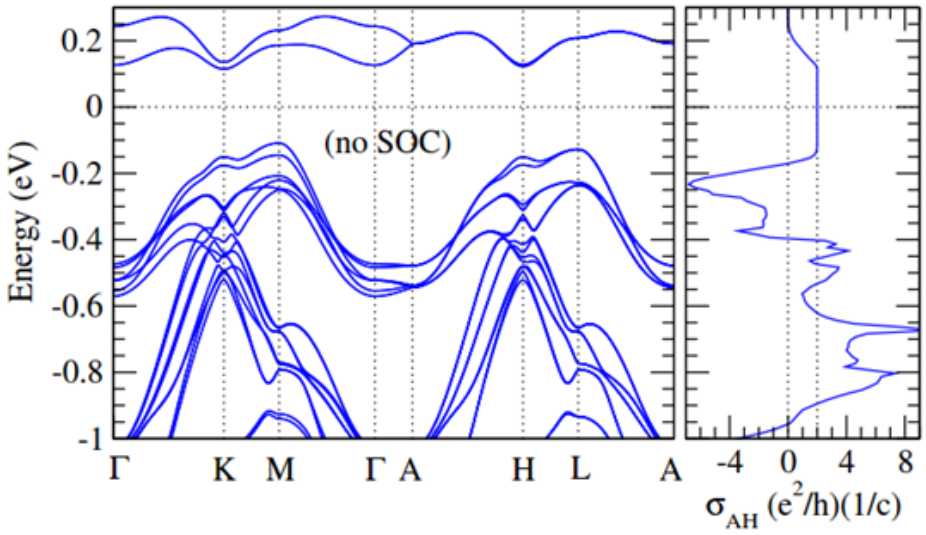

Anomalous Hall conductivity

$$\sigma_{AH} = -\frac{e^2}{\hbar(2\pi)^3}\int d^3k \sum_n f(\varepsilon_n(\mathbf{k}))\Omega_n^z(\mathbf{k})$$

$$\Omega_n^z(\mathbf{k}) = -\sum_{n'\neq n}\frac{2\,\mathrm{Im}\langle \mathbf{k}n|v_x|\mathbf{k}n'\rangle\langle \mathbf{k}n'|v_y|\mathbf{k}n\rangle}{(\omega_{\mathbf{k}n}-\omega_{\mathbf{k}n'})^2}$$

For a 3D Chern insulator, $\sigma_{AH} = n_c \dfrac{e^2}{hc}$

n_c is an integer (Chern number)

nc-AFM state is a QAH phase with $n_c = 2$!

Here, $m_s^{tot} = 0$ and no SOC; thus QAH phase is unconventional.

Total solid angle $\Omega = 4\pi$, Berry phase $\gamma = \Omega/2$,
Chern number $n_c = \gamma/2\pi$, thus, AHC $\sigma_{AH} = 2\ e^2/h$.

So it is the exotic quantum topological Hall effect due to the chiral antiferromagnetic structure!

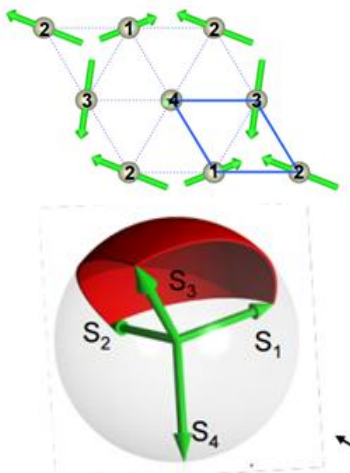

$$\chi = \sum_{ijk}\mathbf{s}_i\cdot(\mathbf{s}_j\times\mathbf{s}_k)$$

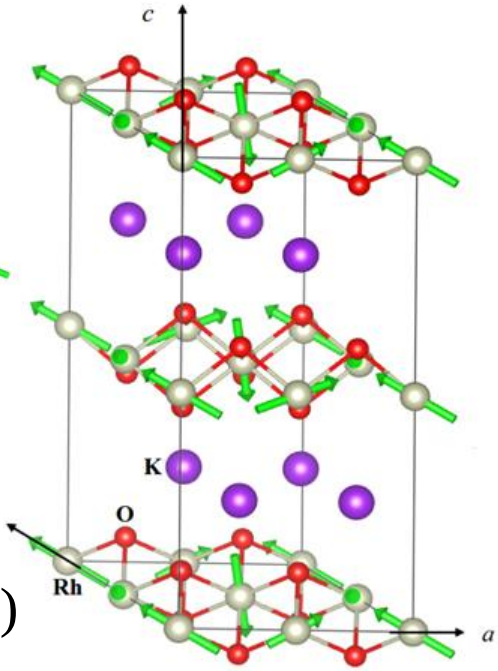

Effects of spin-orbit coupling

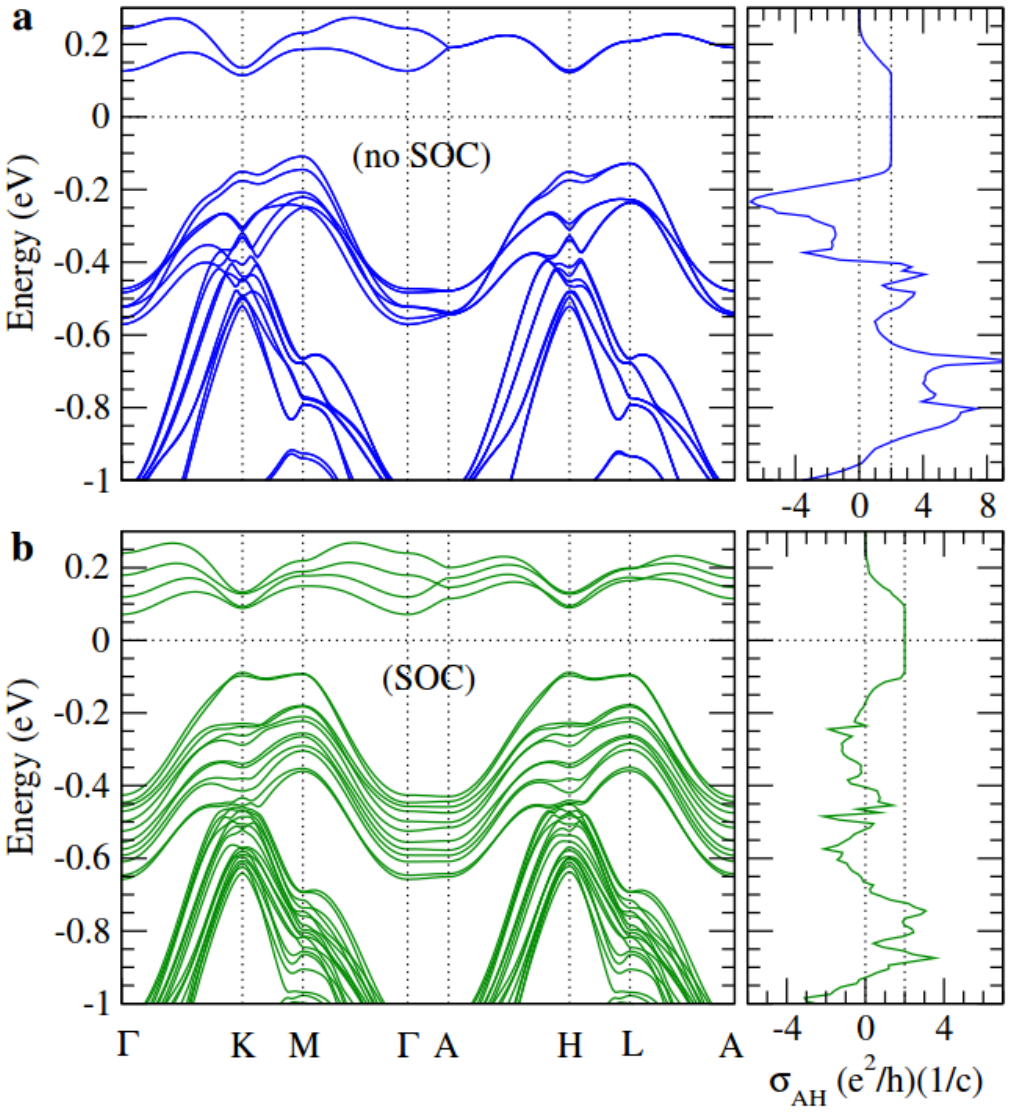

[Zhou et al., PRL 116, 256601 (2016)]

	ΔE^{tot}	m_s^{tot}	m_s^{Rh}	E_g
FM	2.61	0.46	0.33	metal
s-AFM	6.87	0.00	0.22	metal
z-AFM	13.59	0.00	0.21	metal
t-AFM	21.11	0.00	0.10	metal
3:1-FiM	3.55	0.01	0.21	metal
90-c-AFM	2.99	0.00	0.23	0.02
90-nc-AFM	1.90	0.00	0.19/0.22	0.05
nc-AFM	0.00	0.08	0.19/0.24	0.16

The nc-AFM structure remains the lowest energy one and it is still a QAH insulator with E_g = 0.16 eV and m_s^{tot} = 0.08 μ_B/f.u.

III. Topological and chiral phonons in chiral crystals

A. The CoSi family: Unconventional chiral fermion semimetals

The CoSi family (CoSi, CoGe, RhSi, RhGe) has a chiral structure. They were found to host unconventional multifold chiral fermions beyond spin-1/2 Weyl fermions.

[Chang et al., PRL 119 (2017) 206401] [Tang et al., PRL 119 (2017) 206402]

[Kavich et al., Ukr. Fiz. Zh. 23 (1978) 624]

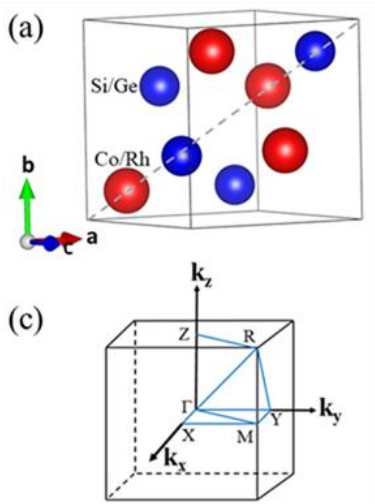

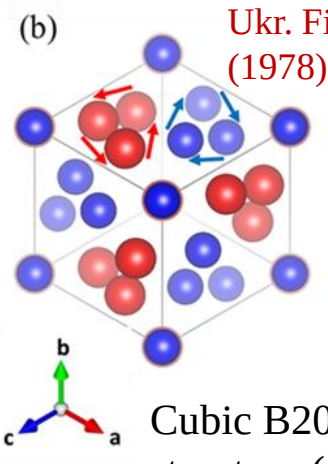

Cubic B20 chiral structure ($P2_13$)

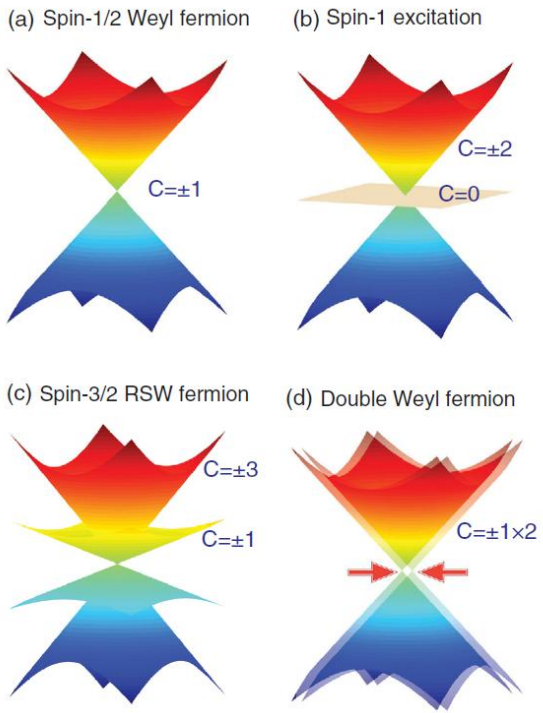

[Tang et al., PRL 119 (2017) 206402]

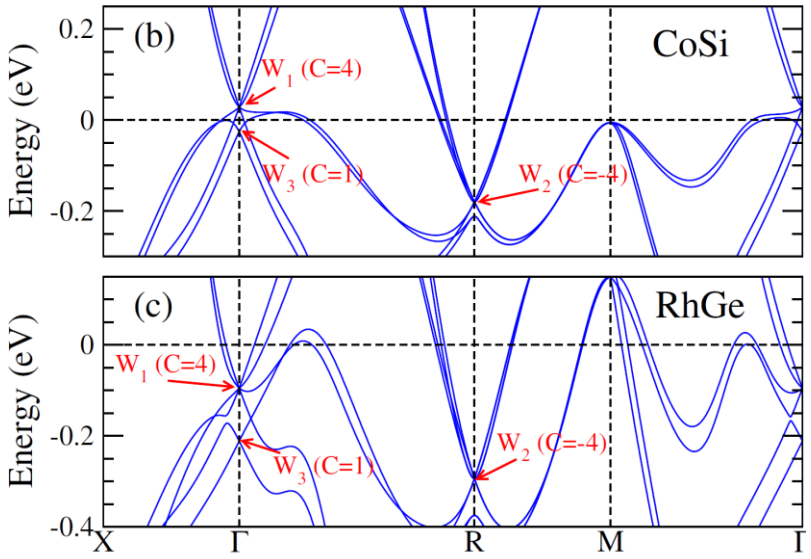

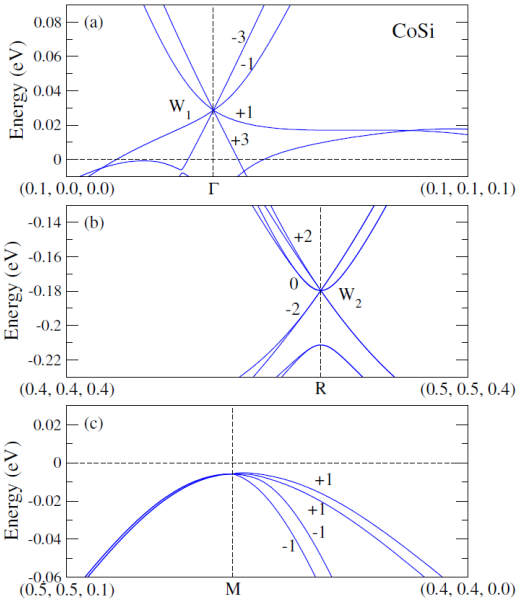

[Hsieh, Prasad, Guo, PRB 106 (2022) 165102]

Thus, the CoSi family has been predicted to exhibit exotic physical properties such as long Fermi surface states, gyrotropic magnetic effect and quantized CPGE.

We have calculated spin Hall effect (SHE) and spin Nernst effect (SNE) and found both SHE and SNE could be helicity-tunable.

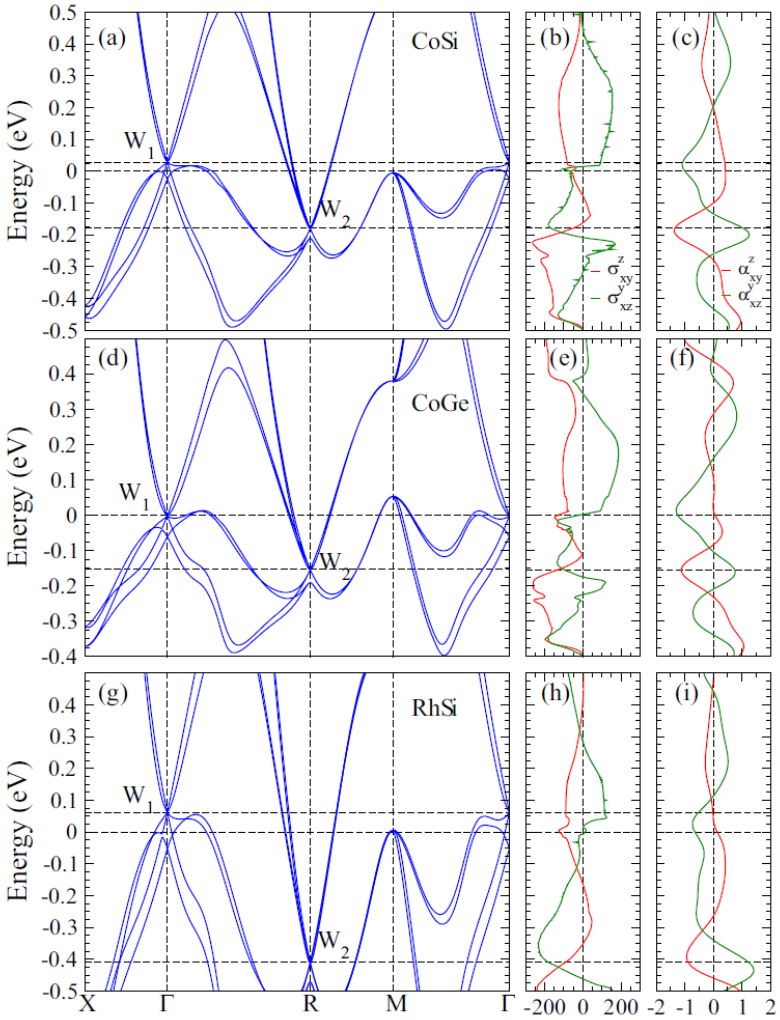

RHC

[Kavich et al., Ukr. Fiz. Zh. 23 (1978) 624]

LHC

[Demchenko et al., Chem. Met. Alloys 1 (1978) 50]

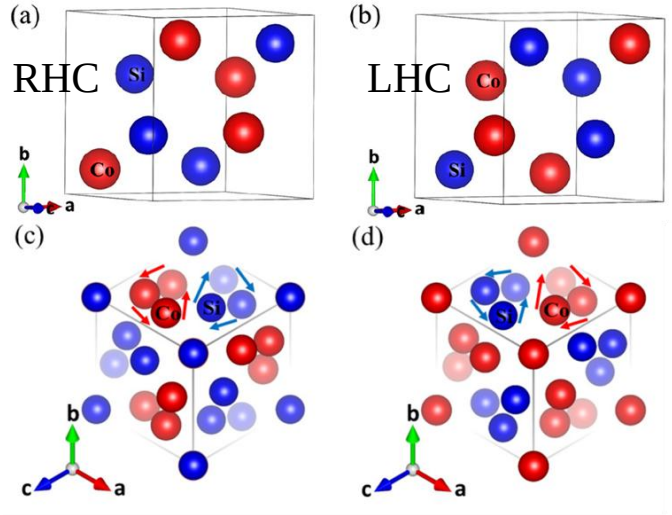

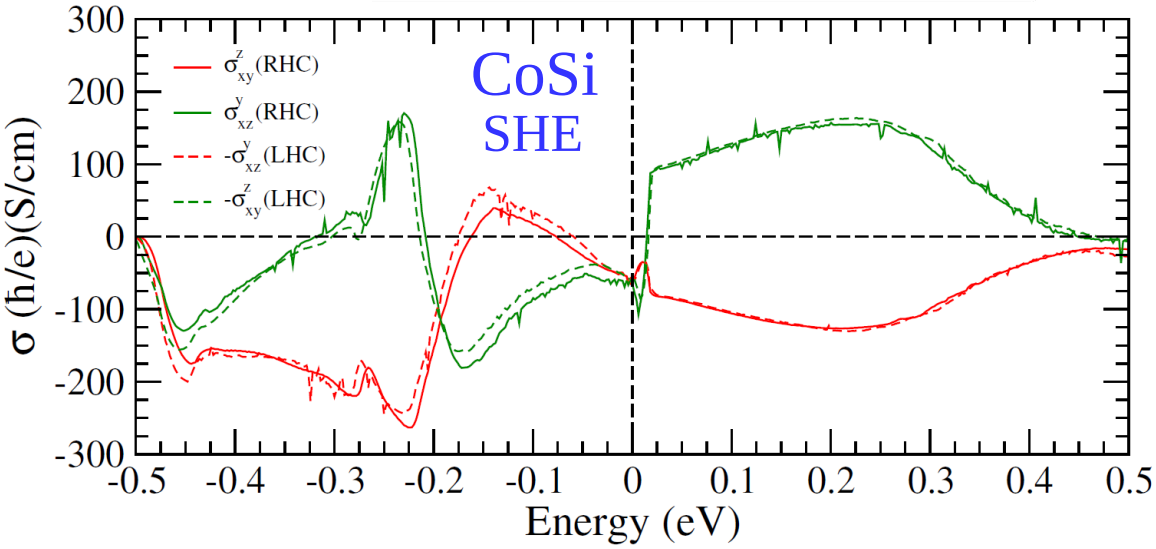

[Hsieh, Prasad, Guo, PRB 106 (2022) 165102]

B. Topological phonons in chiral crystal RhGe

Phonon band structure and topology

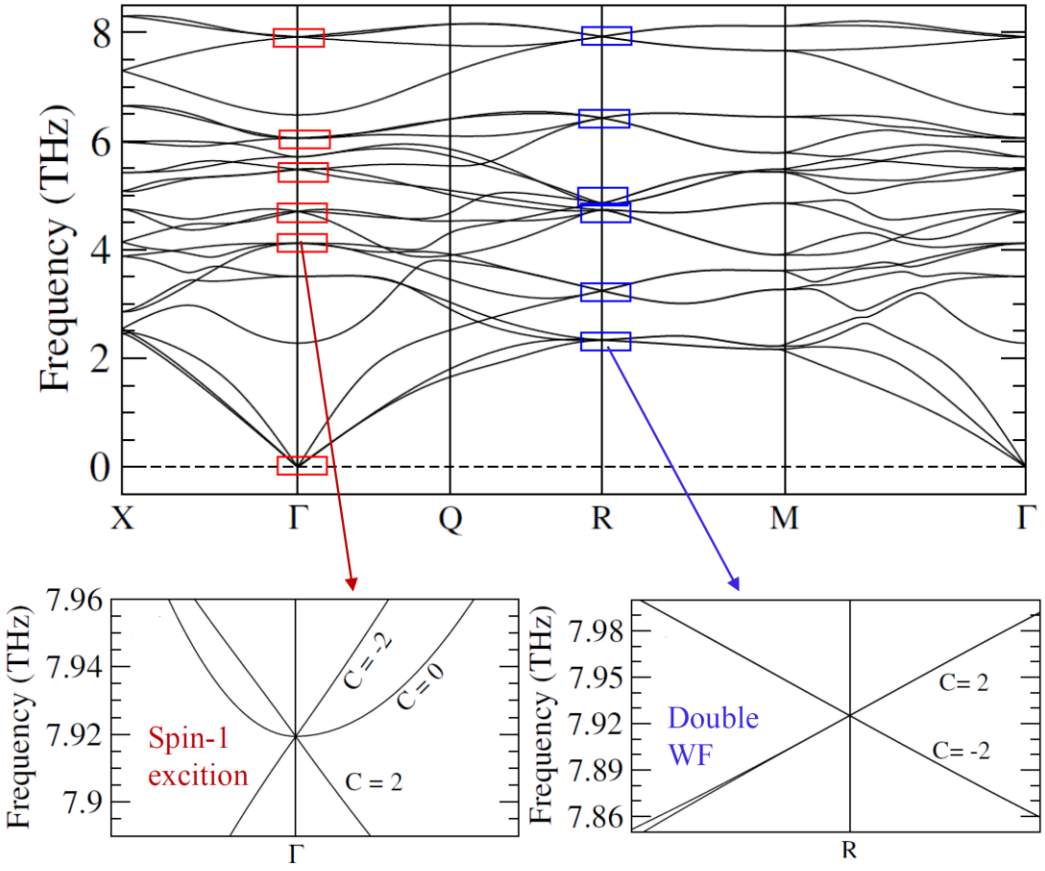

[Reddy, Guo, arXiv: 2410.16000 (2024)]

At the Γ point, Γ_{opt} = 2A + 2E + 5T where A – single, E – double, T – triple degenerate.

	IR				Raman			
WP	A	^{1}E	^{2}E	T	A	^{1}E	^{2}E	T
4a	.	.	.	3	1	1	1	3
Activity	.	.	.	√	√	√	√	√

At the R point, six 4-fold degenerate nodal points which are double Weyl nodes.

Electron band structure and topology

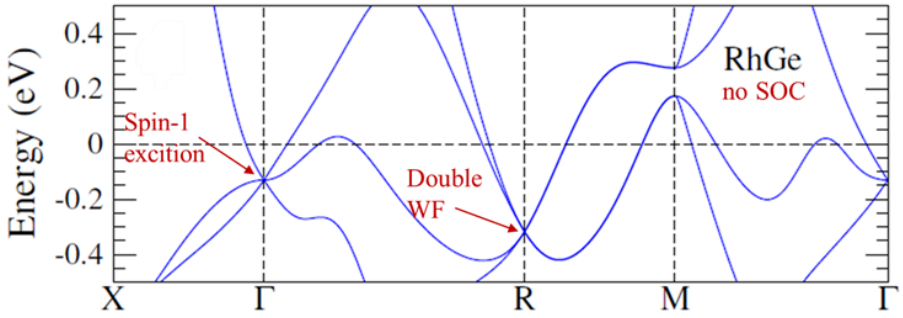

[Hsieh, Prasad, Guo, PRB 106 (2022) 165102]

Conclusion: Topological structure of the phonon bands is identical to that of the electronic band structure without the SOC, because there is no SOC for phonons.

Topological surface states on the (001) surface of RhGe

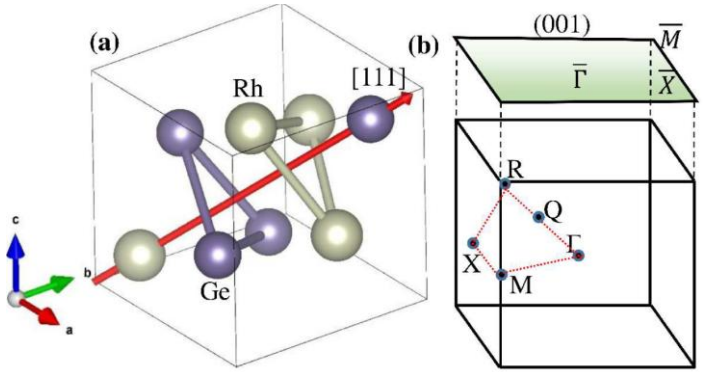

[Reddy, Guo, arXiv: 2410.16000 (2024)]

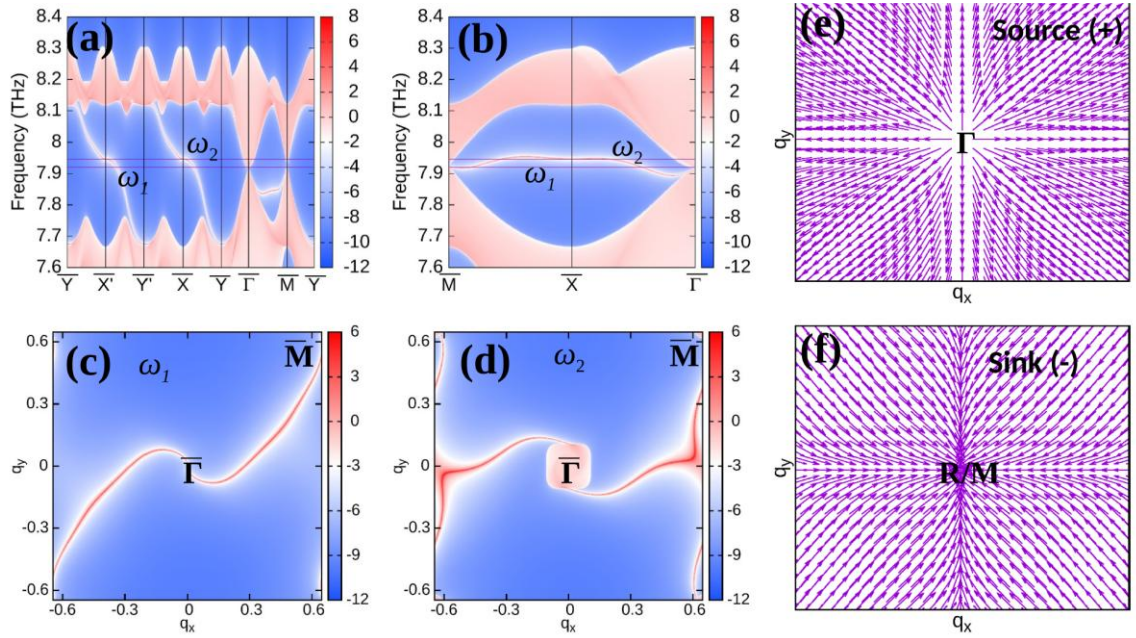

Topological surface states on the (111) surface of RhGe

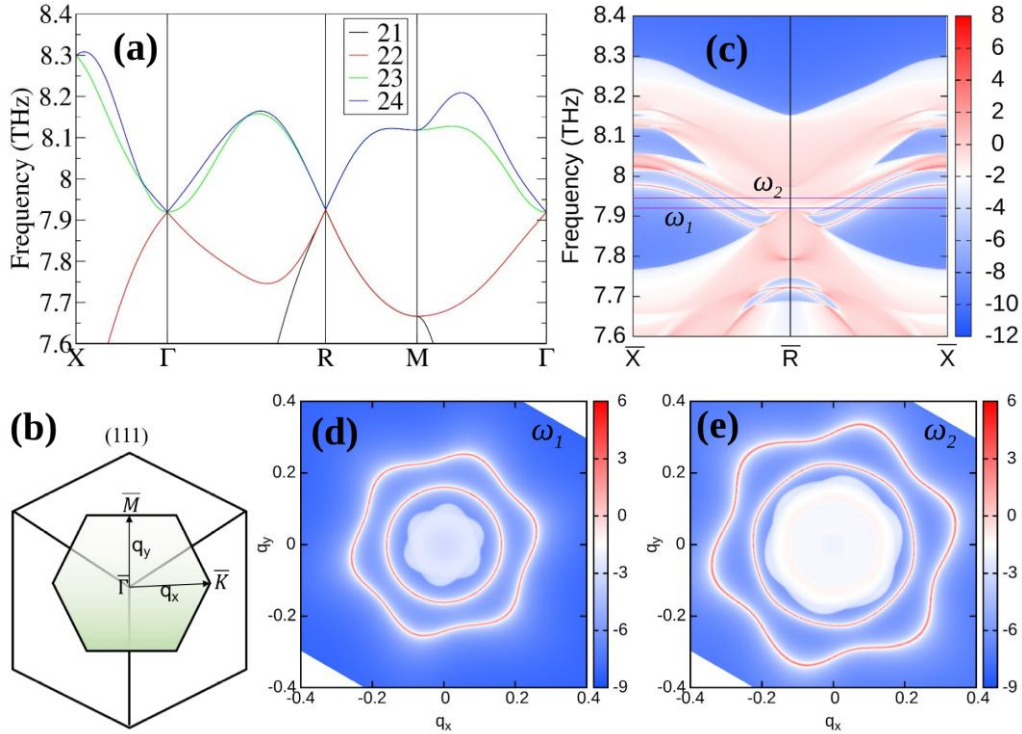

C. Chiral phonon, phonon angular momentum & magnetic moment in RhGe

A characteristic of chiral phonons is their nonzero angular momentum. Thus, figures below show that most phonons in RhGe are chiral phonons. [Reddy, Guo, arXiv: 2410.16000 (2024)]

Phonon mode- and **q**-resolved angular momentum

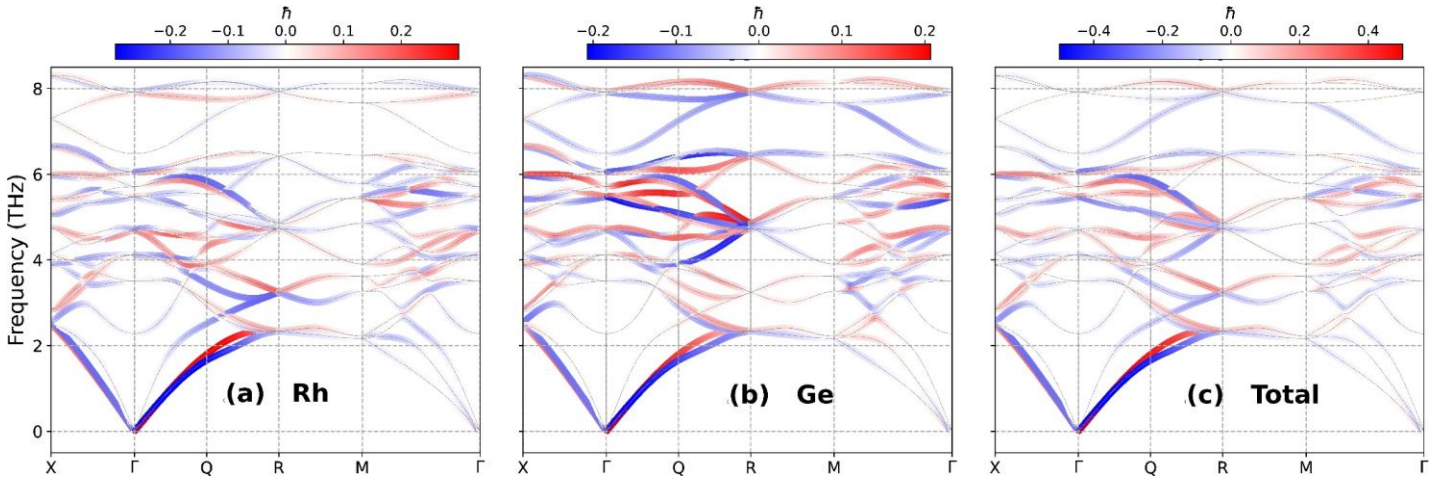

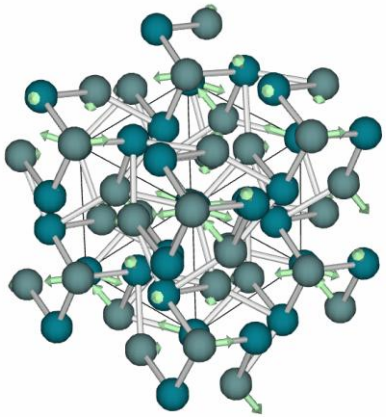

At the +R point (2.336 THz)

Phonon mode- and **q**-resolved magnetic moment

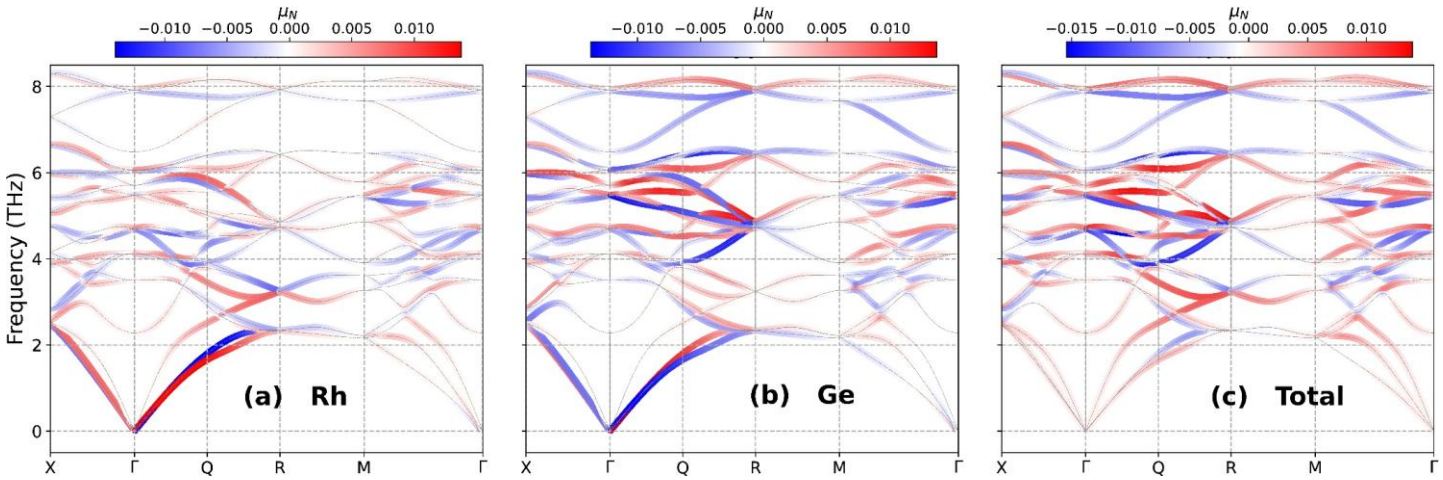

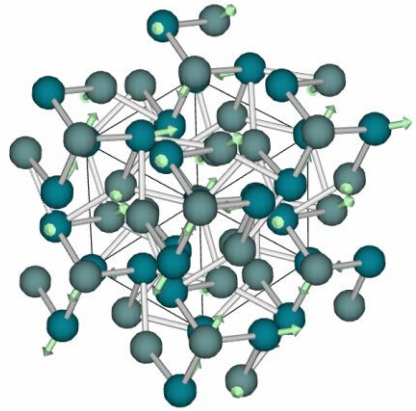

At the -R point (2.336 THz)

[Zhang & Niu, PRL 112 (2014) 085503]

Phonon angular momentum (PAM) $L_\alpha^{ph} = \sum_{j=1}^{N} \sum_{\nu,\mathbf{q}} \left[n_T(\omega_{\nu\mathbf{q}}) + \frac{1}{2} \right] l_{\nu\mathbf{q}}^{j\alpha}$, $\alpha = x, y, z$, Bose function $n_T(\omega_{\nu\mathbf{q}}) = [\exp(\hbar\omega_{\nu\mathbf{q}} / k_B T) - 1]^{-1}$,

and $l_{\nu\mathbf{q}}^{j\alpha} = \sum_{\beta,\gamma} \varepsilon_{\alpha\beta\gamma} \, \mathrm{Im}(e_{j,\nu\mathbf{q}}^{\beta *} e_{j,\nu\mathbf{q}}^{\gamma})$ where $e_{j,\nu\mathbf{q}}^{\gamma}$ are the eigenvectors of the lattice dynamic matrix equation.

Since PAM is zero at Γ and R, we list below PAM and phonon magnetic moment (PMM) at **q**-points near Γ and also at Q.

RhGe: Angular moment (J) and magnetic moment (M) of phonon modes at $\mathbf{q} = (2\pi/a)(0.0025253, 0.0025253, 0.0025253)$ near Γ.

(a) T = 0 K.

Mode	Frequency (THz)	J_{Rh} ($\hbar$)	J_{Ge} ($\hbar$)	J_{RhGe} ($\hbar$)	M_{Rh} (μ_N)	M_{Ge} (μ_N)	M_{RhGe} (μ_N)
1	0.012	0.2931	0.2069	0.5000	-0.0137	0.0137	0.0000
2	0.026	-0.2931	-0.2069	-0.5000	0.0137	-0.0137	0.0000
3	0.044	-0.0000	-0.0000	-0.0000	0.0000	0.0000	0.0000
4	2.281	-0.0008	0.0001	-0.0007	0.0000	0.0000	0.0000
5	3.509	-0.0007	-0.0004	-0.0011	0.0000	-0.0000	0.0000
6	3.509	-0.0007	-0.0004	-0.0011	0.0000	-0.0000	0.0000
7	4.117	0.0078	-0.0058	0.0072	-0.0036	-0.0004	-0.0040
8	4.118	-0.0077	0.0064	-0.0070	0.0036	0.0004	-0.0040
9	4.118	-0.0028	0.0021	-0.0008	0.0001	0.0001	0.0003
10	4.697	0.1331	-0.0804	0.0527	-0.0062	-0.0053	-0.0115
11	4.702	0.0047	-0.0037	0.0010	-0.0002	-0.0002	-0.0005
12	4.707	-0.1308	0.0823	-0.0484	0.0006	0.0054	0.0115
13	5.473	-0.0559	-0.1794	-0.2353	0.0003	-0.0012	-0.0093
14	5.476	-0.0024	0.0031	0.0007	0.0001	0.0002	0.0003
15	5.479	0.0558	0.1709	0.2266	-0.0026	0.0113	0.0087
16	5.711	-0.0019	0.0050	0.0031	0.0001	0.0003	0.0004
17	5.711	-0.0016	0.0056	0.0040	0.0001	0.0004	0.0004
18	6.055	0.1304	0.1175	0.2479	-0.0061	0.0078	0.0017
19	6.056	0.0015	-0.0003	0.0012	-0.0001	-0.0000	-0.0001
20	6.057	-0.1290	-0.1215	-0.2505	0.0060	-0.0008	-0.0020
21	6.482	0.0001	-0.0016	-0.0014	-0.0000	-0.0001	-0.0001
22	7.918	0.0761	-0.0771	-0.0011	-0.0036	-0.0051	-0.0087
23	7.920	-0.0003	0.0004	0.0001	0.0000	0.0000	0.0000
24	7.922	-0.0759	0.0771	0.0013	0.0004	0.0005	0.0087

(b) T = 300 K.

J_{Rh} ($\hbar$)	J_{Ge} ($\hbar$)	J_{RhGe} ($\hbar$)	M_{Rh} (μ_N)	M_{Ge} (μ_N)	M_{RhGe} (μ_N)
304.0170	214.6495	518.6665	-14.1885	14.1905	0.0020
-138.3206	-97.6241	-235.9447	6.4554	-6.4539	0.0015
-0.0005	-0.0005	-0.0010	0.0000	-0.0000	-0.0000
-0.0042	0.0003	-0.0039	0.0002	0.0000	0.0002
-0.0025	-0.0014	-0.0040	0.0001	-0.0001	0.0000
-0.0003	-0.0014	-0.0040	0.0001	-0.0001	0.0000
0.2445	-0.0181	0.2264	-0.0114	-0.0012	-0.0126
-0.0088	0.0065	-0.0024	0.0004	0.0004	0.0008
-0.2409	0.0202	-0.2208	0.0112	0.0013	0.0126
0.3708	-0.2240	0.1468	-0.0173	-0.0148	-0.0321
0.0130	-0.0103	0.0027	-0.0006	-0.0007	-0.0013
-0.3636	0.2289	-0.1347	0.0170	0.0151	0.0321
-0.1357	-0.4357	-0.5715	0.0063	-0.0288	-0.0225
-0.0058	0.0075	0.0017	0.0003	0.0005	0.0008
0.1353	0.4145	0.5498	-0.0063	0.0274	0.0211
-0.0044	0.0118	0.0073	0.0002	0.0008	0.0010
-0.0037	0.1320	0.0095	0.0002	0.0009	0.0010
0.2900	0.2613	0.5513	-0.0135	0.0173	0.0037
0.0032	-0.0007	0.0026	-0.0002	-0.0000	-0.0002
-0.2868	-0.2700	-0.5568	0.0134	-0.0179	-0.0045
0.0003	-0.0033	-0.0030	-0.0000	-0.0002	-0.0002
0.1357	-0.1377	-0.0019	-0.0063	-0.0091	-0.0154
-0.0006	0.0006	0.0001	0.0000	0.0000	0.0001
-0.1353	0.1375	0.0022	0.0063	0.0091	0.0154

RhGe: Angular moment (J) and magnetic moment (M) of phonon modes at Q: $\mathbf{q} = (2\pi/a)(0.25, 0.25, 0.25)$ near Γ.

(a) T = 0 K.

Mode	Frequency (THz)	J_{Rh} ($\hbar$)	J_{Ge} ($\hbar$)	J_{RhGe} ($\hbar$)	M_{Rh} (μ_N)	M_{Ge} (μ_N)	M_{RhGe} (μ_N)
1	1.655	-0.2828	-0.1587	-0.4415	0.0132	-0.0105	0.0027
2	1.801	0.2992	0.1664	0.4656	-0.0140	0.0110	-0.0030
3	2.515	-0.0974	0.0106	-0.0867	0.0045	0.0007	0.0052
4	2.910	0.0123	-0.0402	-0.0278	-0.0006	-0.0026	-0.0032
5	3.034	0.0281	0.0310	0.0591	-0.0013	-0.0020	0.0007
6	3.453	-0.1266	0.0289	-0.0976	0.0059	0.0019	0.0078
7	3.791	-0.0347	0.0064	-0.0283	0.0016	0.0004	0.0020
8	3.894	0.1159	-0.1174	-0.0015	-0.0054	-0.0078	-0.0132
9	3.916	0.0366	-0.0052	0.0314	-0.0017	-0.0003	-0.0020
10	4.307	0.1019	-0.0206	0.0813	-0.0047	-0.0014	-0.0061
11	4.526	0.0509	0.1216	0.1725	-0.0024	0.0080	0.0057
12	4.676	0.0050	0.0104	0.0154	-0.0002	0.0007	0.0004
13	5.012	-0.0359	0.0692	0.0333	0.0017	0.0046	0.0062
14	5.091	-0.0171	-0.1496	-0.1667	0.0008	-0.0099	-0.0091
15	5.543	-0.0013	0.1637	0.1624	0.0001	0.0108	0.0109
16	5.725	0.1320	0.0598	0.1919	-0.0062	0.0039	-0.0022
17	5.852	-0.1765	-0.1206	-0.2971	0.0082	-0.0080	0.0003
18	6.092	-0.0690	0.1365	0.0675	0.0032	0.0090	0.0122
19	6.405	0.0490	-0.1744	-0.1253	-0.0023	-0.0115	-0.0138
20	6.406	0.0090	-0.0204	-0.0113	-0.0004	-0.0013	-0.0018
21	7.254	-0.0132	-0.0568	-0.0700	0.0006	-0.0038	-0.0031
22	7.762	0.0581	-0.0793	-0.0212	-0.0027	-0.0052	-0.0080
23	8.151	-0.0342	0.0778	0.0436	0.0016	0.0051	0.0067
24	8.151	-0.0093	0.0606	0.0513	0.0004	0.0040	0.0044

(b) T = 300 K.

J_{Rh} ($\hbar$)	J_{Ge} ($\hbar$)	J_{RhGe} ($\hbar$)	M_{Rh} (μ_N)	M_{Ge} (μ_N)	M_{RhGe} (μ_N)
-2.1488	-1.2058	-3.3545	0.1003	-0.0797	0.0206
2.0913	1.1628	3.2541	-0.0976	0.0769	-0.0207
-0.4906	0.0536	-0.4370	0.0229	0.0035	0.0264
0.0540	-0.1757	-0.1217	-0.0025	-0.0116	-0.0141
0.1179	0.1302	0.2481	-0.0055	0.0086	0.0031
-0.4698	0.1074	-0.3624	0.0219	0.0071	0.0290
-0.1181	0.0218	-0.0963	0.0055	0.0014	0.0069
0.3840	-0.3889	-0.0049	-0.0179	-0.0257	-0.0436
0.1206	-0.0170	0.1036	-0.0056	-0.0011	-0.0067
0.3073	-0.0621	0.2453	-0.0143	-0.0041	-0.0184
0.1467	0.3504	0.4971	-0.0068	0.0232	0.0164
0.0140	0.0292	0.0432	-0.0006	0.0019	0.0013
-0.0943	0.1818	0.0875	0.0044	0.0120	0.0164
-0.0444	-0.3873	-0.4317	0.0021	-0.0256	-0.0235
-0.0031	0.3931	0.3900	0.0001	0.0260	0.0261
0.3082	0.1396	0.4479	-0.0144	0.0092	-0.0052
-0.4043	-0.2762	-0.6803	0.0189	-0.0183	0.0006
-0.1526	0.3019	0.1494	0.0071	0.0200	0.0271
0.1039	-0.3696	-0.2657	-0.0048	-0.0244	-0.0293
0.0191	-0.0432	-0.0240	-0.0009	-0.0028	-0.0037
-0.0252	-0.1087	-0.1339	0.0012	-0.0072	-0.0060
0.1052	-0.1438	-0.0385	-0.0049	-0.0095	-0.0144
-0.0597	0.1358	0.0761	0.0028	0.0090	0.0118
-0.0162	0.1057	0.0895	0.0008	0.0070	0.0078

IV. Crystal chirality-induced magneto-optical effects in collinear antiferromagnets

A. Crystal chirality-driven anomalous Hall effect in, e.g., RuO_2

The AHE in ferromagnetic metals has been attributed to the nonzero magnetization and SOC. Thus, no AHE would be expected in simple collinear antiferromagnets because of zero net magnetization and Kramers spin degeneracy.

In antiferromagnetic bcc Cr, e.g., though T-symmetry is broken, ($R + T$) (e.g., $\tau_{1/2}T$ or PT) remains symmetric. Consequently, Kramers theorem remains valid and Berry curvature is identically zero in the **k**-space. Therefore, no AHE could occur.

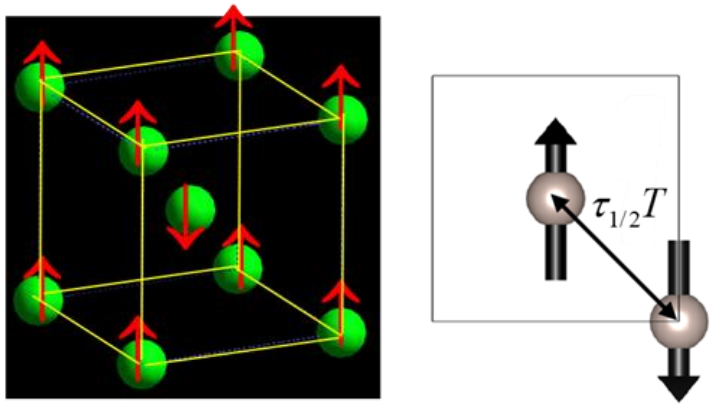

BCC antiferromagnetic Cr

RuO_2 has a tetragonal structure with P-symmetry ($P4_2/mnm$) (a). Ru atoms sit on a tetragonal lattice (b) and thus in the antiferromagnetic state, there is $\tau_{1/2}T$ symmetry. However, O atoms sit on the noncentrosymmetric positions and have local crystal chirality $\boldsymbol{\chi} = \mathbf{d}_{AO} \times \mathbf{d}_{OB}$.

[Šmejkal et al., Sci. Adv. 6, eaaz8809 (2020)]

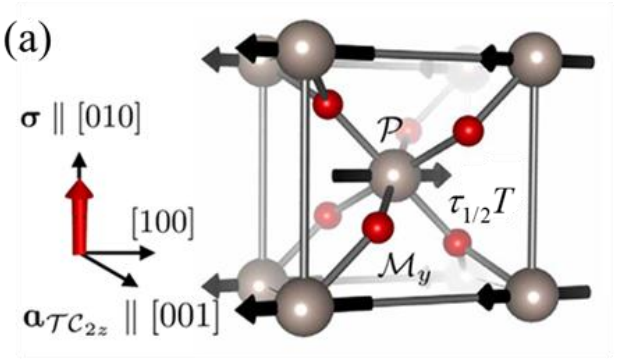

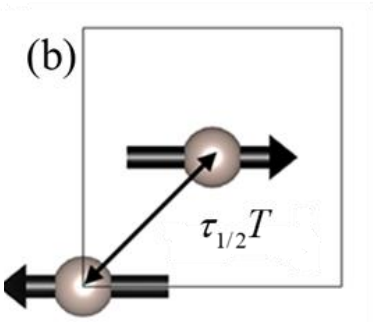

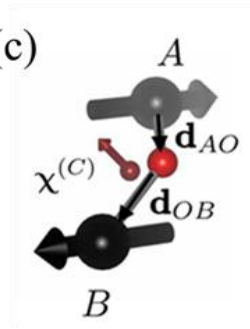

Collinear antiferromagnetic RuO_2

This crystal chirality breaks $\tau_{1/2}T$-symmetry and lifts Kramers spin degeneracy, thus leading to AHE in AFM RuO_2.

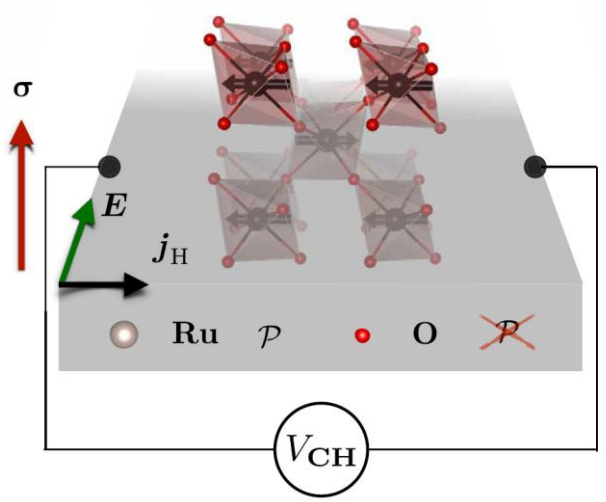

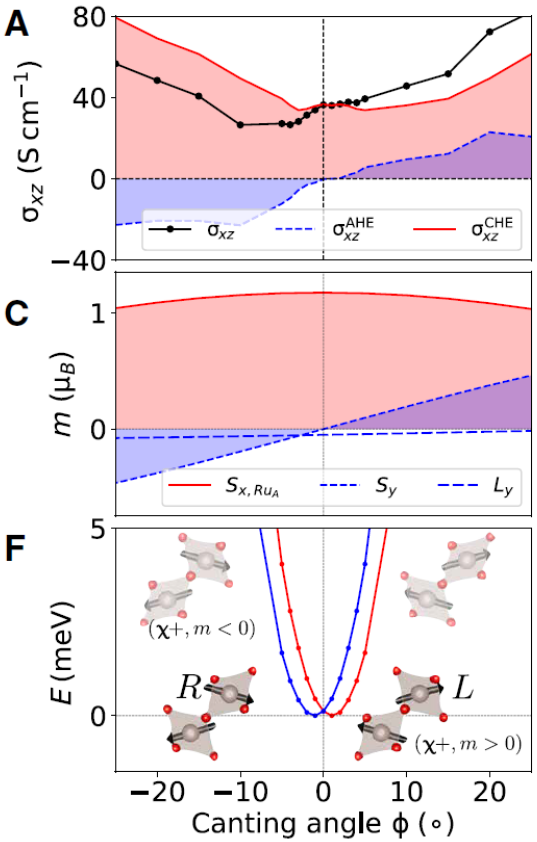

B. Magneto-optical effect in collinear antiferromagnets RuO_2 and $CoNb_3S_6$

1. Predicted magneto-optical effects in antiferromagnets RuO_2

Theoretical calculations: [Zhou et al., PRB 104 (2021) 024401]

(1) Using the experimental structure; (2) GGA+U method, with U_{Ru} = 2 eV.

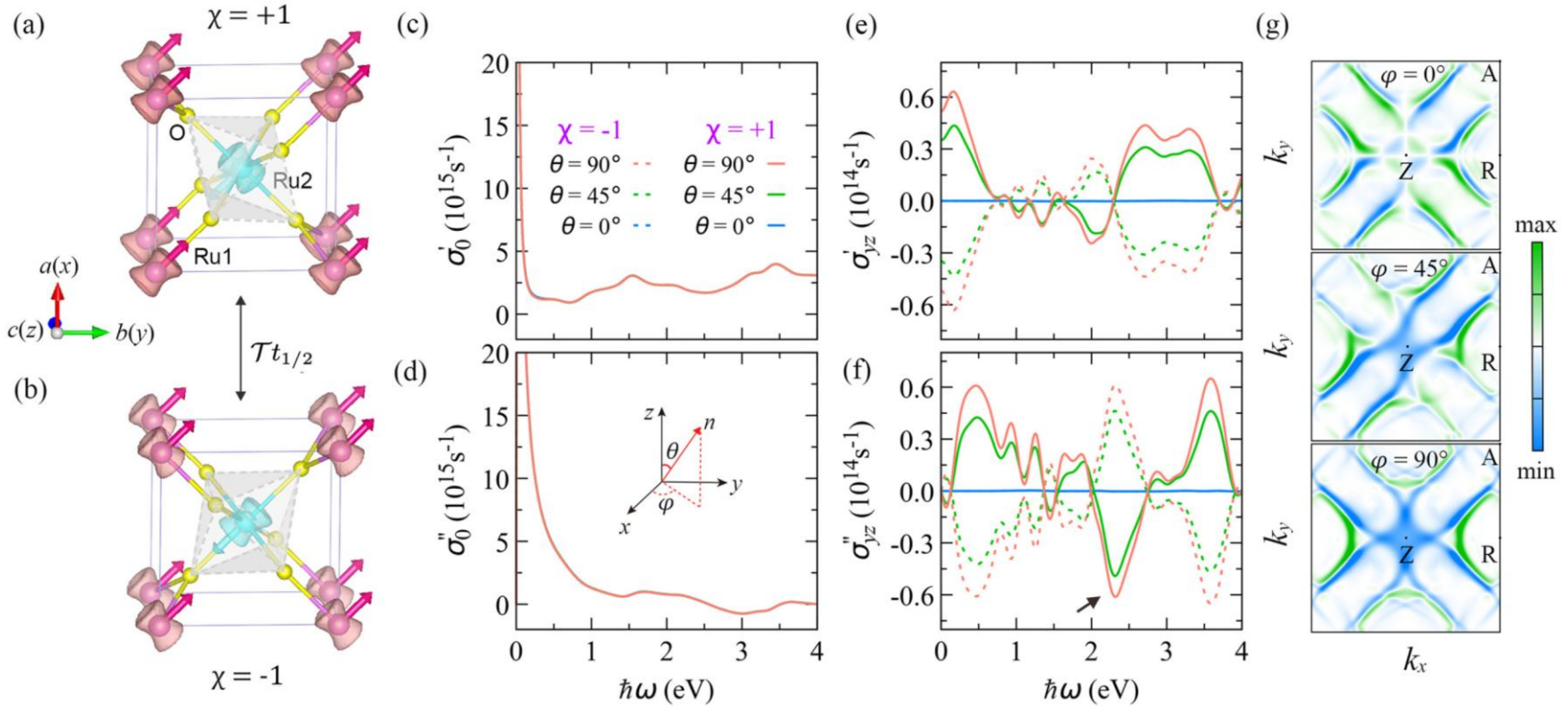

(a-b) Crystal structures of RuO_2. (c-d) Diagonal optical conductivity. (e-f) Off-diagonal optical conductivity. (g) Momentum resolved σ_{yz}'' for χ = +1 at photon energy of 2.31 eV.

Rotations (a) (c) and ellipticities (b) (d) of the magneto-optical Kerr (a-b) and Faraday (c-d) effects of RuO_2.

[Zhou et al., PRB 104 (2021) 024401]

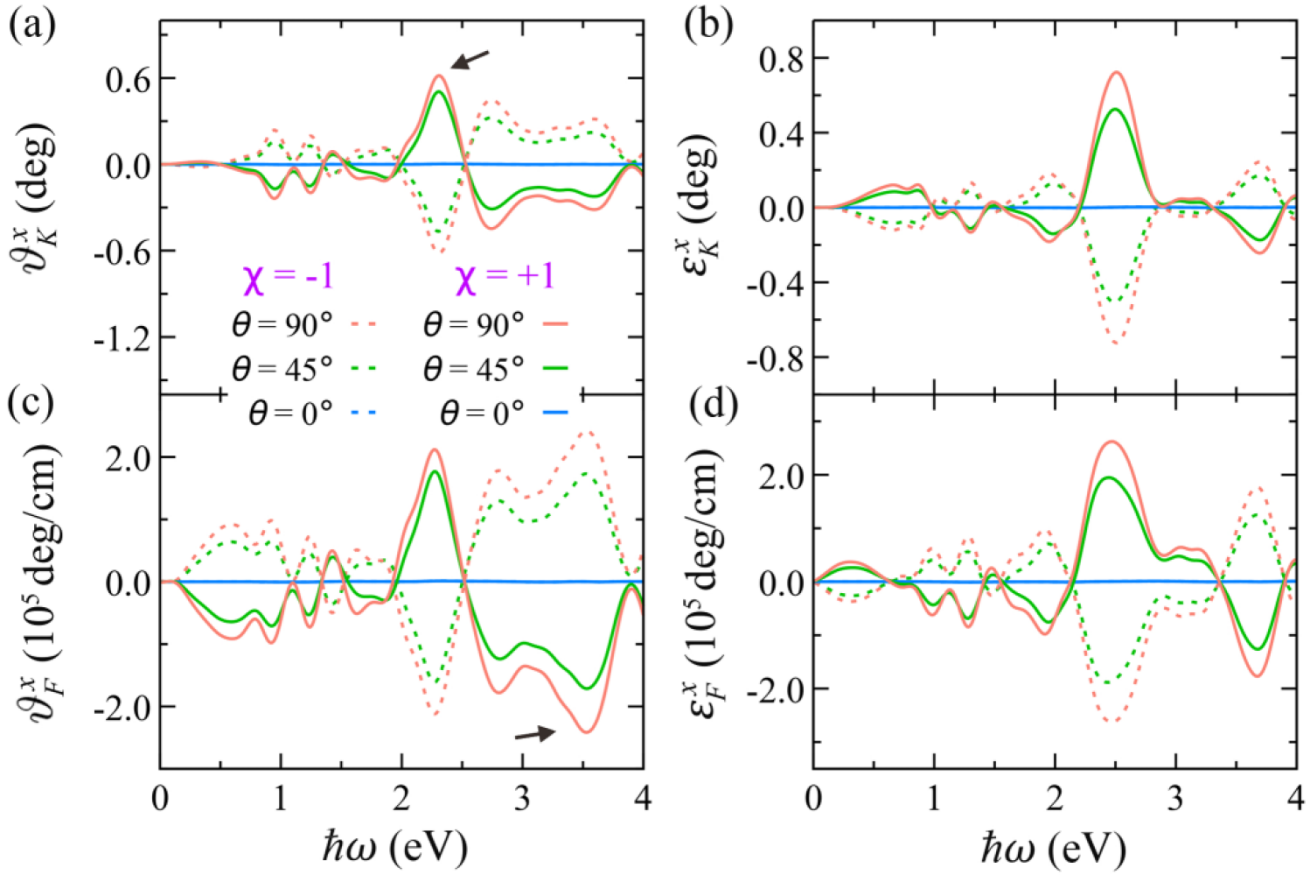

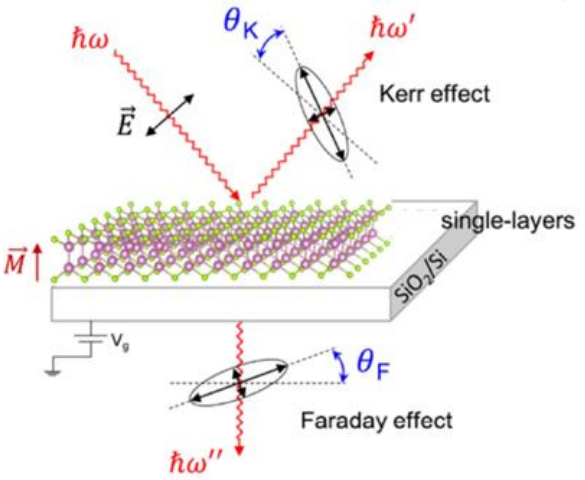

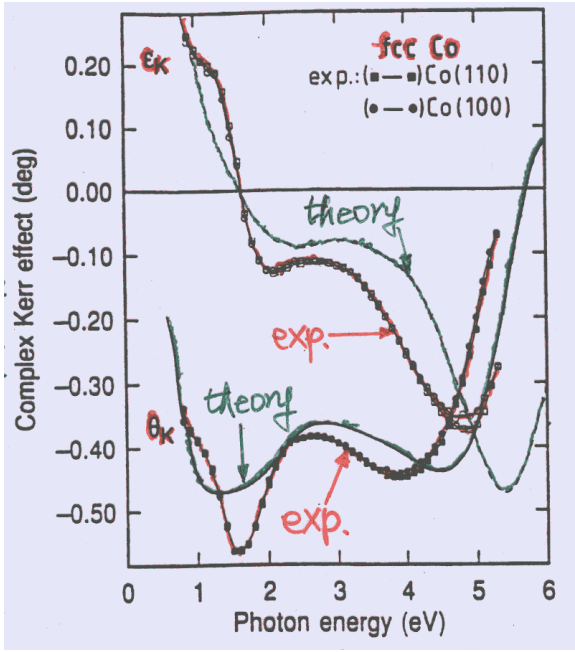

[Guo, Ebert, PRB 50, 10377 (1994)]

2. Predicted magneto-optical effect in collinear antiferromagnet $CoNb_3S_6$

(i.e., intercalated TMD $Co_{1/3}NbS_2$)

Layered $CoNb_3S_6$ is the Co-intercalated 2H NbS_2 ($Co_{1/3}NbS_2$). Co atoms form a collinear antiferromagnetic state below 25 K (b). Pristine 2H NbS_2 has a centrosymmetric hexagonal structure ($P6_322$) (a). However, antiferromagnetic $CoNb_3S_6$ is noncentrosymmetric and, furthermore, is a chiral crystal ($P6_322$). Therefore, the combination of the global crystal chirality and broken T symmetry would lift Kramers spin degeneracy and thus would result in nonzero anomalous Hall effect and magneto-optical effects in $CoNb_3S_6$.

[Parkin, Marseglia, Brown, J. Phys. C 16 (1983) 2765]

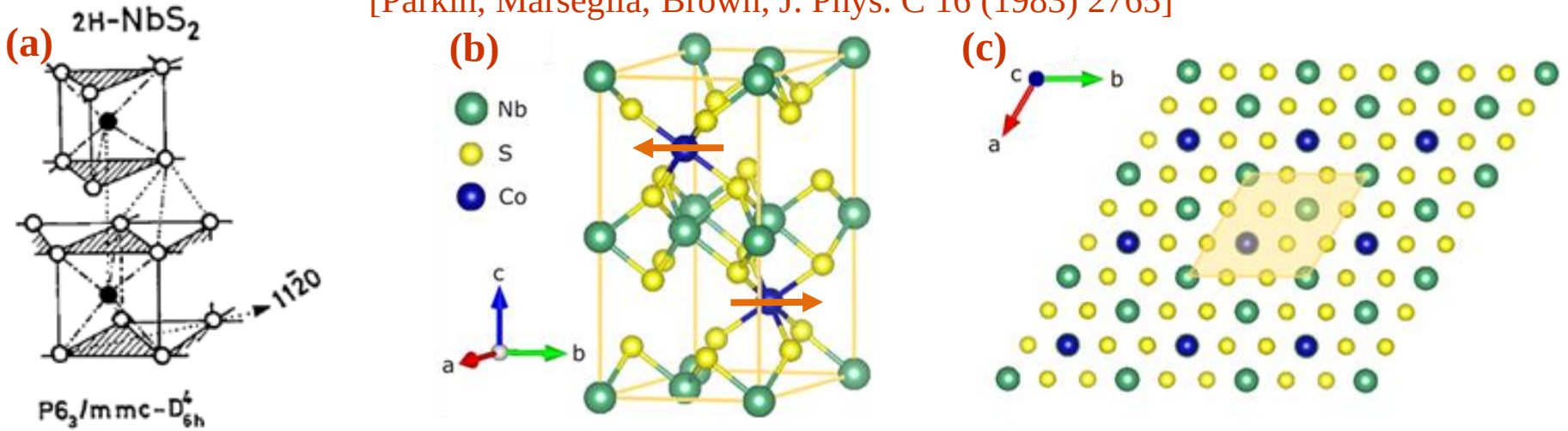

Chiral crystalline structure of $CoNb_2S_6$ with χ = -1 (a) and χ = +1 (b).

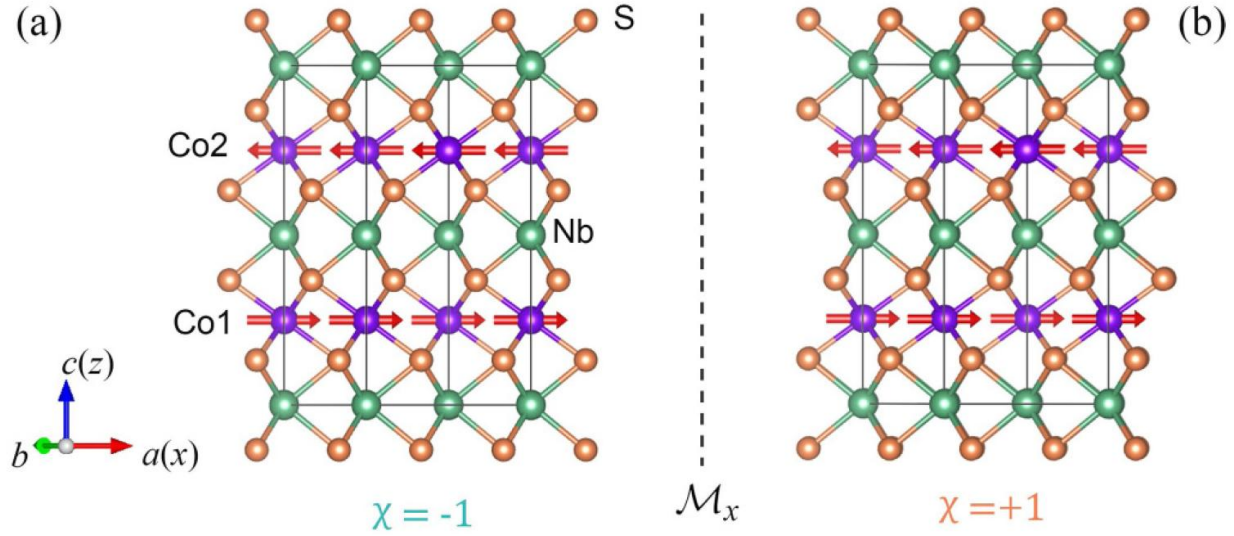

Theoretical calculations: (1) Using the experimental structure; (2) GGA+U method, with U_{Co} = 4 eV.

Calculated Kerr (c) and Faraday (d) rotations of $CoNb_2S_6$.

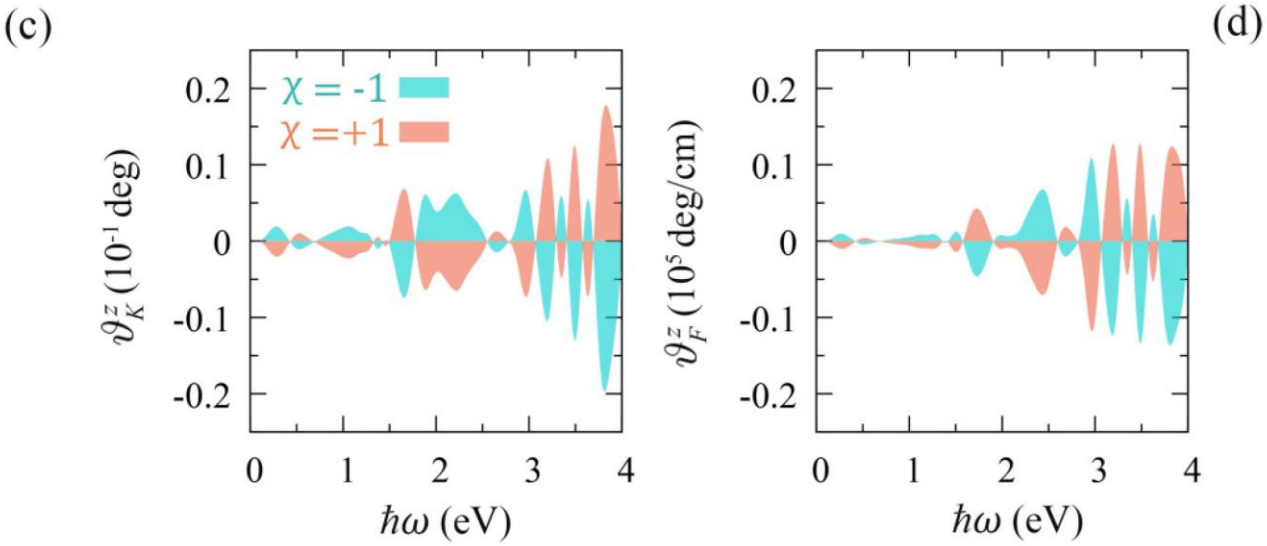

C. Post-publication notes

(1) Recent μSR experiments showed that bulk RuO_2 is nonmagnetic (e.g., [Hiraishi et al., PRL 132 (2024) 166702]).

(2) Latest experiments indicate that the antiferromagnetic state in $CoNb_3S_6$ is noncoplanar instead of collinear one. The large observed topological Hall effect is due to the scalar spin chirality of noncoplanar spin structure.

(3) Nevertheless, the (local) crystal chirality mechanism of the anomalous Hall effect and magneto-optical effects should still work in other collinear antiferromagnets with crystal chirality (e.g., Mn_5Si_3 and MnTe).

(4) In 2022, a collinear antiferromagnet with crystal chirality was coined an altermagnet [Šmejkal et al., PRX 12 (2022) 040501], which has become a hot research topic ever since.

Large THE & TNE in noncoplanar antiferromagnet $CoNb_3S_6$.

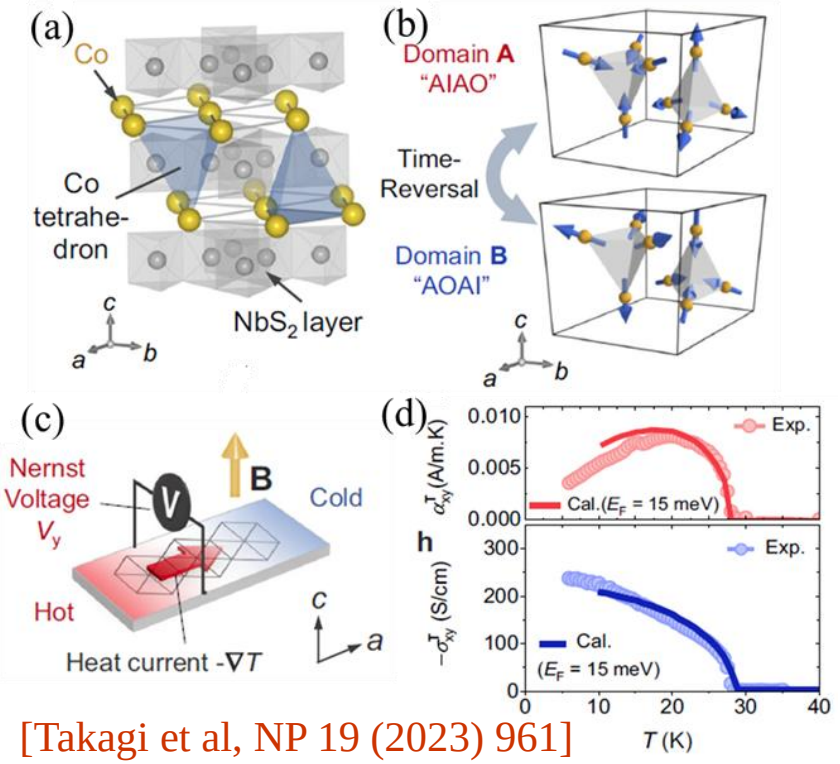

[Takagi et al, NP 19 (2023) 961]
[Khanh et al, NC 16 (2025) 2654]

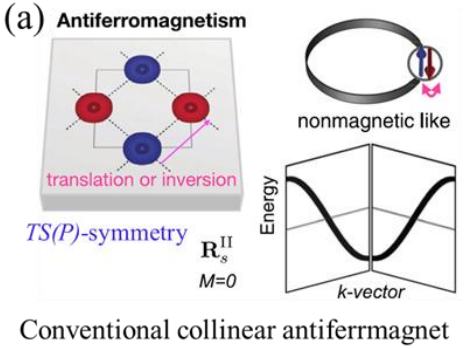

Conventional collinear antiferrmagnet

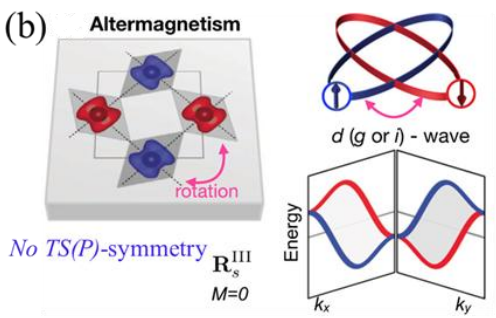

Collinear antiferrmagnet with crystal chirality

V. Summary

Chirality (handedness) in crystal and spin structures can cause unexpected phenomena in solids.

In particular, scalar spin chirality in a noncoplanar antiferromagnet (e.g., $K_{1/2}RuO_2$) could result in the exotic quantum topological Hall phase in the system.

Crystal chirality could enable a chiral metal to host unconventional multifold chiral quasiparticles in both electronic band structure and phonon band structure of the solid.

Both global and local crystal chirality could cause unexpected anomalous Hall effect and magneto-optical effect in collinear antiferromagnets with zero net magnetization.

Acknowledgements

Discussion and Collaboration

Jian Zhou and his team (Nanjing U.)
Wanxiang Feng, Yugui Yao and their team (BIT)
Qian Niu (USTC)
P. V. Sreenivasa Reddy (Nat'l Taiwan U.)

Support

NSTC 國家科學及技術委員會
National Science and Technology Council

NCTS

Thank you for your attention!